Journal of Earth Science, *Vol. 29*, *No. 4*, *p. 806–823*, *August 2018* *ISSN 1674-487X*
Printed in China
https://doi.org/10.1007/s12583-018-0787-3

Western Tethyan Epeiric Ramp Setting in the Early Triassic: An Example from the Central Dinarides (Croatia)

Dunja Aljinović[1], **Micha Horacek**[2], **Leopold Krystyn**[3], **Sylvain Richoz**[4], **Tea Kolar-Jurkovšek**[5], **Duje Smirčić**[*1], **Bogdan Jurkovšek**[5]

1. *University of Zagreb*, *Faculty of Mining*, *Geology and Petroleum Engineering*, *Pierottijeva* 6, *Zagreb* 10000, *Croatia*
2. *BLT Wieselburg*, *HBLFA Francisco-Josephinum*, *Rottenhauserstr.* 1, *Wieselburg* 3250, *Austria*
3. *Institute of Paleontology*, *Vienna University*, *Althanstraße* 14, *Vienna* 1090, *Austria*
4. *Lund University*, *Lithosphere and Biosphere science*, *Sölvegatan* 12, *Lund* 22362, *Sweden*
5. *Geological Survey of Slovenia*, *Dimičeva Ulica* 14, *Ljubljana* 1000, *Slovenia*

Dunja Aljinović: https://orcid.org/0000-0002-4698-1727; Duje Smirčić: https://orcid.org/0000-0002-6360-8203

ABSTRACT: In the central part of the External Dinarides in Plavno, Croatia, near Knin, a remarkably thick (927.5 m) Early Triassic depositional sequence was investigated. The Plavno sequence starts in the EarlyGriesbachian and ends with a continuous transition into the Anisian strata. A complete ^{13}C isotope curve has been achieved and combined with conodonts, bivalves and ammonoids to establish and correlate stage and substage boundaries. The $\delta^{13}C$ curve is consistent with former studies. It displays a general increase from the Griesbachian to a prominent maximum beyond the +8‰ amplitude around the Dienerian-Smithian boundary (DSB), followed by a steep and continuous decline to low, negative values in the Smithian. Around the Smithian-Spathian boundary (SSB) a steep rise to a second maximum occurred. It is followed by a saw-tooth shaped decline in the Spathian and a similar increase to a peak at the Spathian-Anisian boundary (SAB).

Sedimentologically, the Plavno sequence is interpreted as having been deposited on an extensive epeiric ramp under long-term transgressive conditions, sharing depositional characteristics of both the epeiric platform and the carbonate ramp. The entire Plavno sequence was deposited above the storm-wave base and was storm influenced. Three informal members are differentiated: 1) the dolostone member (Early Griesbachian); 2) the siliciclastic member (red-coloured shale, siltstone, sandstone with oolitic/bioclastic grainstone intercalations), which can be further divided into lower, middle and upper intervals (Late Griesbachian, Dienerian and Smithian); and 3) the mudstone member (grey lime mudstones, marls and calcisiltites with common ammonoids and gastropods-Spathian). The Plavno sequence is compared with other western Tethyan sections. Observed differences stem from local controls on deposition in the overall shallow marine environment.

KEY WORDS: Early Triassic, Dinarides, epeiric ramp, $\delta^{13}C$ isotope curve, litho- and biostratigraphy.

0 INTRODUCTION

The continuous, almost complete and enormously thick (~1 000 m) Early Triassic sequence of Plavno, Croatia, near Knin (a central part of the External Dinarides), represents the very important locality in a Dinaridic region documenting the Early Triassic sedimentary evolution of the western Tethys margin. It is thus a key area for comparison with the intensively studied Early Triassic sequences in the Southern Alps in Italy, and the Transdanubian and Bükk Mountains in Hungary (e.g., Brandner et al., 2012; Kovács et al., 2010; Hips and Pelikán, 2002; Rüffer and Zühlke, 1995; De Zanche et al., 1993; Krainer, 1993; Perri, 1991; Broglio Loriga et al., 1986, 1983 and references therein) to reveal more about lateral and vertical continuity; similarities and differences in the lithozones and biofacies zones; and the lithostratigraphy between these neighbouring areas.

Lower Triassic rocks of the External Dinarides extend through Slovenia, Croatia, Bosnia and Herzegovina, and Montenegro (Fig. 1) and have been studied by many authors (Krystyn et al., 2014; Kolar-Jurkovšek et al., 2011a; Aljinović, 1997, 1995; Herak et al., 1983; Šćavničar and Šušnjara, 1983; Ivanović et al., 1978; Grimani et al., 1975, 1972). Lithostratigraphic nomenclature of Lower Triassic rocks in the Dinarides was traditionally based on the Alpine Region—Dolomites and Northern Calcareous Alps, (Herak et al., 1983) following the historic division of the Werfen Formation into two lithostratigraphic units: the lower "seiser schichten" and the upper

*Corresponding author: dsmircic@rgn.hr

Manuscript received July 27, 2017.
Manuscript accepted March 29, 2018.

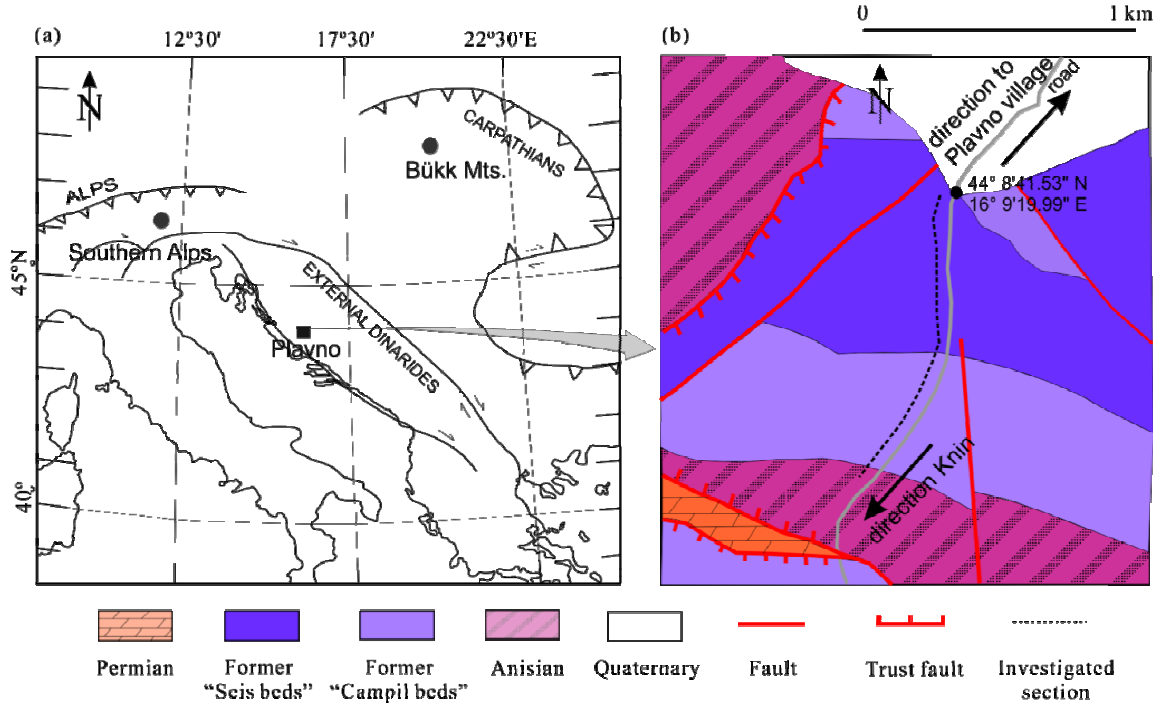

Figure 1. (a) Regional map showing the general location of the Southern Alps, Bükk Mts. and the Plavno Section; (b) geological map of the Plavno Section (modified after Grimani et al., 1972).

"campiler schichten" (Bauer et al., 1983; Von Richthofen, 1860; Wissmann and Münster, 1841). These two Early Triassic units were also used during mapping of the Plavno area and the External Dinarides (e.g., Grimani et al., 1975, 1972 shown in Fig. 2). Due to the alleged similarity with the Werfen beds of the Dolomites, Herak et al. (1983) proposed the Muć Section (~ 60 km SE of Plavno) as the "Upper Scythian" standard for the Werfen facies. However, the Werfen Formation of the dolomites is still divided into nine members based on the contributions of many geologists (e.g., De Zanche et al., 1993, 1980; Assereto et al., 1973; Bosellini, 1968, 1964). Additionally, palaeontological research by Broglio Loriga et al. (1986, 1983) documented a significantly different age for the South Alpine Seis and Campil Member than the historically-used age associated terms "Seis beds" and "Campil beds." For the Dinarides, this historical nomenclature continued until recently, when Aljinović et al. (2011) declined usage of the Italian definitions when referenced within the Croatian part of the Dinarides. Aljinović et al. (2011) noted that the Dinaridic "Seis" and "Campil beds" as lithostratigraphic units have a different chronostratigraphic meaning with respect to their Italian counterparts. Similar conclusions were also previously made by Herak et al. (1983), who implied that the Campil Member of the Werfen facies in the Southern Alps was older than the investigated "Campil beds" (Unit B) of the Muć Section.

Biostratigraphic constraints for the Lower Triassic rocks in the Croatian part of the External Dinarides are typically obtained from macrofossils such as bivalves and ammonoids, but rarely from microfossils such as conodonts (Aljinović et al., 2011, 2006; Jelaska et al., 2003; Herak et al., 1983). The characteristic bivalve genus *Claraia* has been reported from the "Seis beds" in the Gorski Kotar region (e.g., Herak et al., 1983; Babić, 1968; Đurđanović, 1967). Spathian ammonoids have been described by Krystyn (1974) and Golubić (2000) from the "Campil beds" of Muć.

More recently, sedimentary features and biostratigraphy of the Early Triassic strata were documented at several localities: Gorski Kotar (Aljinović et al., 2006, 2005), Plavno and Bosansko Grahovo (Aljinović et al., 2011; Aljinović, 1995). At Gorski Kotar, the depositional environment has been interpreted as a storm influenced shallow marine shelf with carbonate oolitic barrier bar interval (*parvus-isarcica* Zones) overlain by mixed siciliclastic-oolitic facies (*obliqua* Zone) of the inner shelf. The vertical change of facies was interpreted as a consequence of transgression that led to widening and development of shallow epicontinental sea.

The Early Triassic deposits of the Plavno Section were previously investigated for sedimentology (Aljinović, 1995) and biostratigraphy (Aljinović et al., 2011). Aiming to provide more exact sedimentological, litho-, bio-, and chemostratigraphic constraints, we reinvestigate the Plavno succession, and include a summary of our palaeontological and stable isotopic results. With this new lithostratigraphic and sedimentologic data, we aim to correlate the Plavno sequence with the Early Triassic sequences in the Southern Alps (Dolomites, Italy), Hungary (south of the Inner Western Carpathians Bükk Mts. and Central Transdanubia) and other parts of the External Dinarides.

1 GEOLOGICAL SETTING

The Dinarides are classically subdivided into the Internal and External Dinarides. The fold belt striking along the coast of the Adriatic Sea has been termed the External Dinarides subunit (Herak, 1986). It consists predominantly of Jurassic and Cretaceous carbonates (Vlahović et al., 2005). Palaeozoic and Triassic rocks crop out in anticlinal or thrust-related struc-

tures (Chorowitz, 1977; Grimani et al., 1975, 1972; Herak, 1973). Consequently, the Early Triassic Plavno sequence described in Fig. 1 is part of an overturned SW limb of a NW-SE striking anticline formed in hanging wall of a NE dipping thrust fault. The Plavno Section is located some 2 km to the west of the village after which it is named (Fig. 1) and is perfectly exposed along the road leading to Knin (Fig. 1). Less than 10% of the nearly 1 000 m thick section is covered. The beds are vertical and steeply overturned. The start of the section is at 44°8'41.53"N, 16°9'19.99"E.

Šćavničar and Šušnjara (1983), Tišljar (1992) and Herak (1973) documented a trend of tectonic uplift at the end of Permian and beginning of the Early Triassic. This uplift generated a hypersaline sea with very low relief (Herak, 1973) and evaporitic coastal sabkhas (Tišljar, 1992). The contact between the Permian and Lower Triassic rocks has been debated (Grimani et al., 1975; Ivanović et al., 1971), though it is generally considered conformable and is usually complicated by tectonics and younger diapiric phases of Permian evaporites.

2 METHODS

Petrography and facies analysis were performed at the University of Zagreb, Faculty of Mining, Geology and Petroleum Engineering. A total of 126 thin sections were analysed using a polarized microscope after a staining procedure with Alizarin Red S and K-ferricyanide.

Fifty of the 92 total conodont samples proved to be productive. The positions of the samples containing time diagnostic conodonts are shown in Figs. 2 and 3. The rock samples weighed 2–4 kg were processed at the Geological Survey of Slovenia using standard laboratory techniques.

More than 190 samples were collected along the entire section for the carbon isotope analysis. The hand specimens were cut and inspected for weathered surfaces and other altered areas, which were avoided during sampling. Micrite rich layers were preferred for the isotope analysis. Sampling was conducted using a dental micro-drill. Sample powders were reacted with 100% phosphoric acid at 70 °C in a Kiel II automated reaction system, and the evolved carbon dioxide gas was

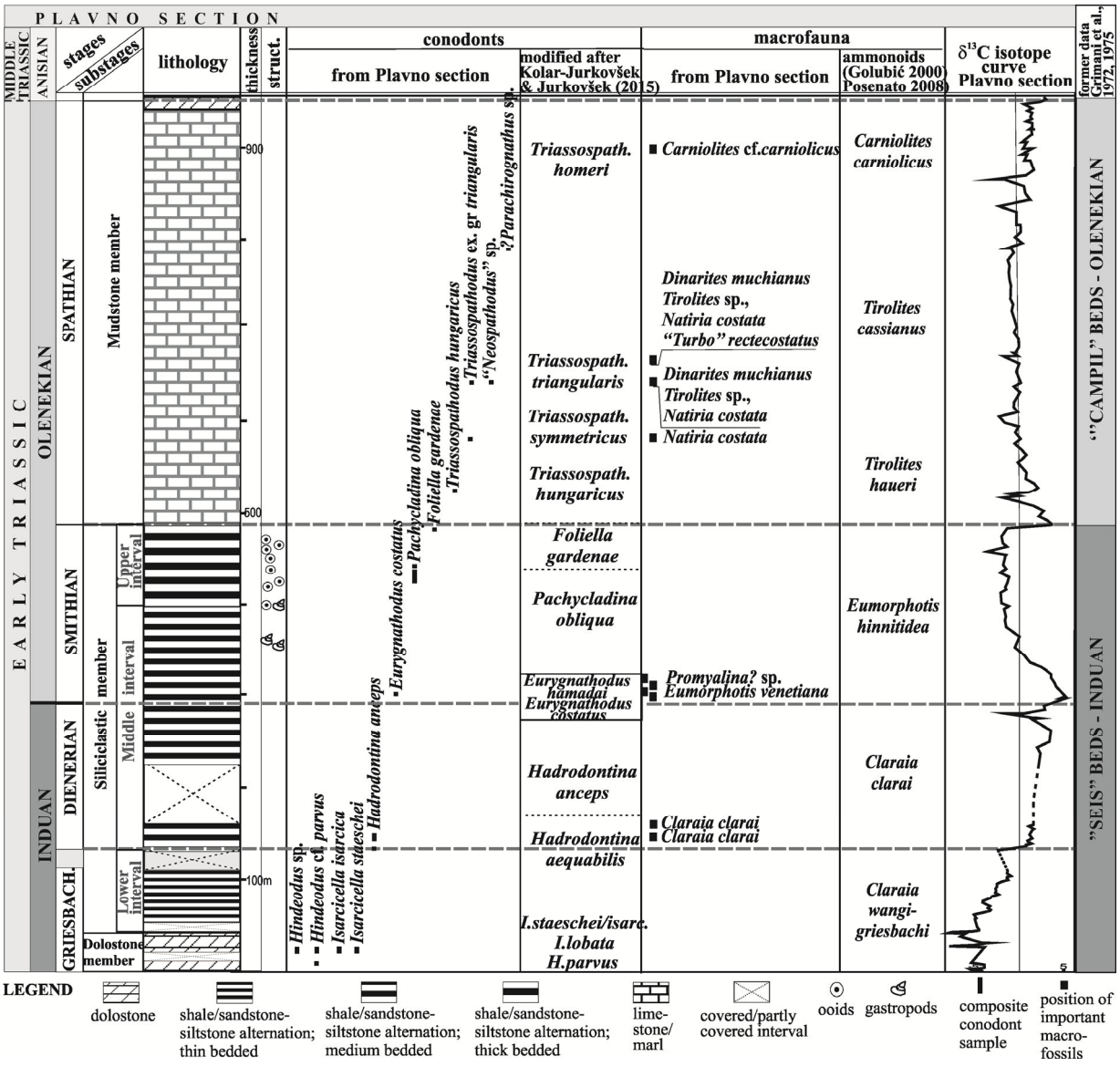

Figure 2. Simplified column of the Plavno Section with major stratigraphic divisions according to lithology, conodonts, macrofossils and C-isotope curve.

analysed with a Finnigan Delta Plus mass spectrometer at the University of Graz (analytical precision, 1 : <0.05‰ for $\delta^{13}C$, <0.1‰ for $\delta^{18}O$). The $\delta^{13}C$ and $\delta^{18}O$ values were corrected according to the NBS19 standard and reported in per mill (‰) relative to the Vienna-peedee belemnite (V-PDB) standard. ^{18}O results were not corrected for the different fractionation factor of dolomite.

3 STRATIGRAPHY

3.1 Chemostratigraphy ($\delta^{13}C$ Isotope Curve)

Along the section, a continuous $\delta^{13}C$ isotope curve was produced (Figs. 2 and 3; Supplement 1). By comparing the Early Triassic $\delta^{13}C$ isotope curve from successions in Italy, China, Iran and many other regions (e.g., Clarkson et al., 2013; Grasby at al. 2012; Sun et al., 2012; Horacek et al., 2009, 2007a, b; Payne et al., 2006; Richoz, 2006), chemostratigraphic stage and sub-stage boundaries were possible to propose. In the basal Griesbachian strata, the trend of the $\delta^{13}C$ isotope curve remains at low values (~ -3.5‰), followed by a steady increase toward -1.5‰. Near the assumed Griesbachian-Dienerian boundary a minor negative excursion (~1‰) has been noticed, which is consistent with other regions (e.g., Horacek et al., 2007b). In the Dienerian strata, the ^{13}C-values increase with several short, negative inflections and a steepening of the slope toward the Dienerian-Smithian boundary (DSB), as seen in many other sections (e.g., Clarkson et al., 2013; Romano et al., 2013; Song et al., 2012; Horacek et al., 2010, 2009, 2007a, b; Richoz, 2006; Payne et al., 2004). Around DSB, a prominent maximum of +5.2‰ occurs, followed by a steep and continuous drop to low, negative values (-2‰ to -1‰) in the Smithian. This trend is also visible in numerous other sections (e.g., Sun et al., 2015; Clarkson et al., 2013; Romano et al., 2013; Song et al., 2012; Horacek et al., 2010, 2009, 2007a, b; Payne et al., 2004). Right before the Smithian-Spathian boundary (SSB), a steep rise to a second maximum of +5.6‰ occurs. This is followed by a declining saw-tooth pattern in the Spathian (between -2‰ and -1‰) and an increase to a third positive maximum at +3.4‰ around the Spathian-Anisian boundary (SAB).

The curve presented in this study (Figs. 2, 3) is generally more negative than most other published curves, especially during the Griesbachian (e.g., Clarkson et al., 2013; Romano et al., 2013; Song et al., 2012; Horacek et al., 2010, 2009, 2007a, b; Richoz, 2006; Payne et al., 2004), but the trends are easily recognized and correlated. However, the values of the dolostone member should be taken with caution, as they may have been altered (Fig. 4a) during dolomitization. Usually Early Triassic dolomitic samples record the marine $\delta^{13}C$-patterns as reliably as calcite samples (previously demonstrated for many sections, e.g., Horacek et al., 2010, 2007a, b). However, in the cited literature early/primary dolomite was mostly present. For late diagenetic dolomite, the situation might be different. Read et al. (2016) managed to demonstrate a high stability of $\delta^{13}C$ in dolomite despite variations in $\delta^{18}O$ and Sr-content and isotopes due to dolomitization.

3.2 Biostratigraphy (Conodonts, Bivalves, Ammonoids)

Conodonts from the Plavno Section are rather rare and of moderate preservation (the determined taxa listed in Supplement 2). Yet, the fauna enabled determination of a few diagnostic elements. The basal-most sample, PL 01, yields only fragments of *Hindeodus* sp. On the other hand, the Sample PL 03/04 is characterized by the presence of *Hindeodus parvus* (Kozur and Pjatakova), *Isarcicella isarcica* (Huckriede) and *I. staeschei* (Dai and Zhang), thus marking the *isarcica-staeschei* Zone (Figs. 2 and 3). The co-occurrence of these taxa in the lowermost part of the *isarcica-staeschei* Zone coincides with the conodont zonation proposed by Kolar-Jurkovšek and Jurkovšek (2007) for the Lukač Section (Slovenia). Samples PK 23, T 17 and T 17a contain *Eurygnathodus costatus* (Staesche) and *E. hamadai* (Koike), which are indicative of the basal Smithian strata (Horacek et al., 2015; Krystyn et al., 2004; Payne et al., 2004). In Sample PK 40a presence of *Foliella gardenae* (Staesche) marks a top-Smithian (Kolar-Jurkovšek and Jurkovšek, 2015; Figs. 2 and 3). Samples PK 48 through PK 66 bear the youngest conodonts from the Spathian genus *Triassospathodus* (*T.* ex gr. *hungaricus* (Kozur and Mostler) *T.* ex gr. *triangularis* (Bender)) (Figs. 2 and 3).

Biochronologically significant macrofossils are extremely rare in the lower part of the section (Figs. 2 and 3). Single occurrences of *Claraia clarai* (Emmr.) are important in proving the Dienerian age for beds T 5a and T 6. Bivalves from the Smithian part (*Eumorphotis venetiana* (Hauer), *Promyalina*) have limited stratigraphic value. Ammonoids occur exclusively in the Spathian part of the sequence within two widely separated intervals. The first level (T 81b), which is approximately 157 m above Smithian-Spathian boundary, contains *Dinarites muchianus* (Hauer) and *Tirolites* sp., and is indicative of EarlySpathian strata. The second horizon (T 116) with *Carniolites* cf. *carniolicus* (Mojsisovics), located more than 200 m higher up section, exhibits a Late Spathian strata (Figs. 2 and 3). Conodont taxa are listed in Supplement 2 and illustrated in Supplement 3.

4 LITHOLOGY AND DEPOSITIONAL ENVIRONMENT

The Plavno sequence is subdivided into three well-differentiated units—informal members: (1) the dolostone member (Early Griesbachian); (2) the red siliciclastic member (shale, siltstones and sandstones—Late Griesbachian), with upward-occurring intercalation of bioclastic calcarenites and ooid grainstones (Dienerian and Smithian); and (3) the grey mudstone member, with alternating lime mudstones, marls and calcisiltites (Spathian) (Figs. 2 and 3). In Aljinović et al. (2011) equivalents of the mudstone member were two-fold divided (mudstone versus siltstone-mudstone facies), due to an overall dominance of mudstone vs. siltstone. We merged these two facies into a single unit. The most significant lithofacies features, including occurrence, sedimentary structures, composition, diagenetic features and depositional setting are listed in Table 1.

4.1 Dolostone Member

The Early Griesbachian dolostone member is represented by a ~40 m thick succession consisting of pale yellow dolostone, sandy/silty dolostone and rare limestone. The middle part of the member is covered by vegetation. The dolostone is

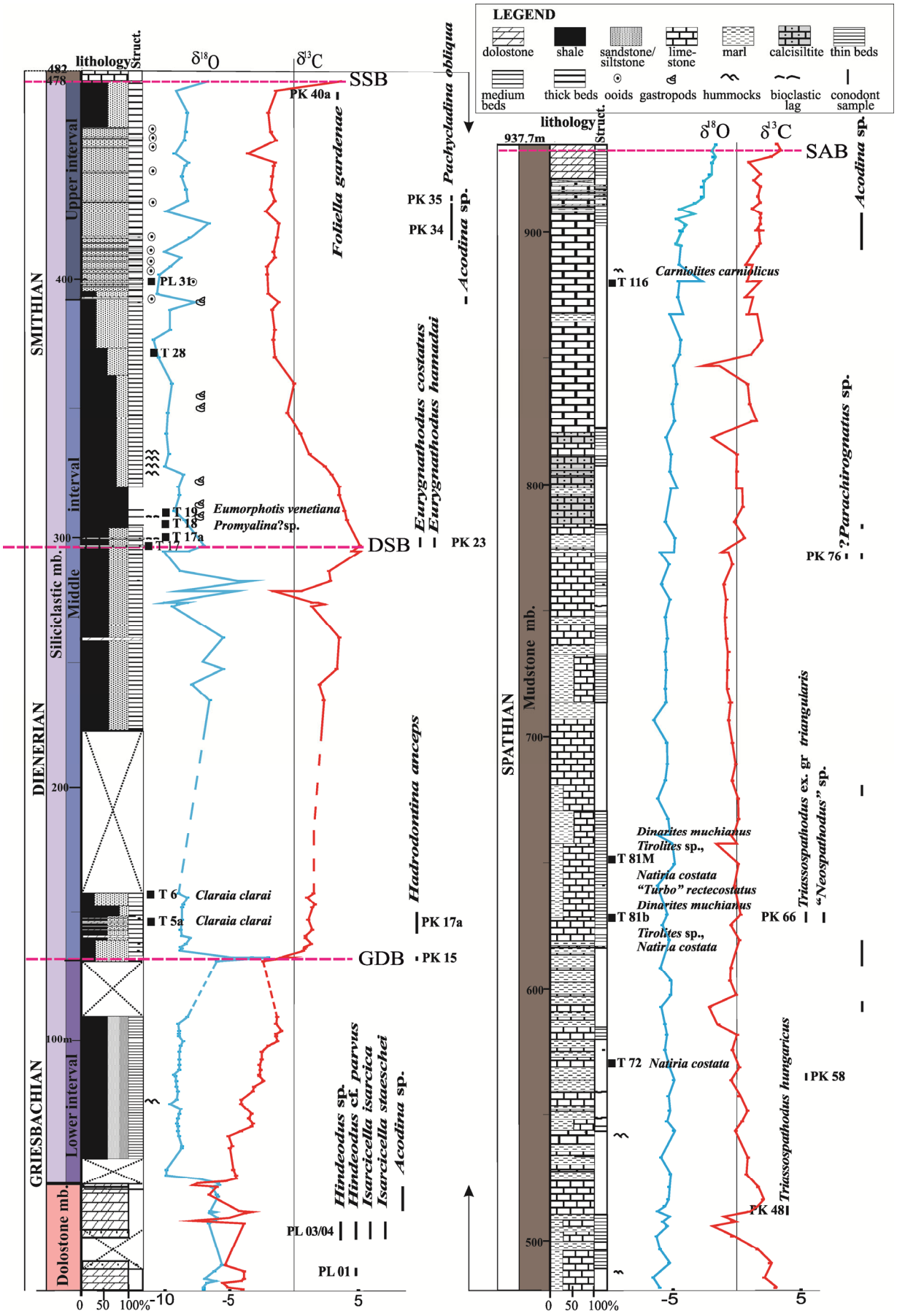

Figure 3. Plavno sequence, C-isotope curve and fossil assemblage of the Plavno succession.

Table 1 Sedimentological characteristics of the differentiated members of the Plavno Section

Units	Dolostone member (0–52 m)	Siliciclastic member			Mudstone member (478–937 m)
		Lower interval (52–130 m)	Middle interval (130–395 m)	Upper interval (395–478 m)	
Stratigraphy	Lower Griesbachian	Upper Griesbachian	Upper Dienerian–Lower Smithian	Upper Smithian	Spathian
Occurrence	Pale yellow dolostone, subordinate sandy/silty dolostone; rare limestone	Gray or yellow shales, siltstones and sandstones;	Red shales, siltstones and sandstones; Rare intercalation of dolostones, bioclastic and oolitic/oncolitic calcarentites -upward increasing amount of shales	Red siltstones and sandstones; Intercalations of oolitic grainstones -Upward increasing amount of siltstone/sandstone component	Gray lime mudstones and marls
Sedimentary structures	-Thick bedded, massive	-Thin-bedded (3–10 cm) -Mostly planar beds -Lateral variation in bed thickness (pinch and swell geometry); -Horizontal planar lamination or ripple cross-lamination; -Symmetric wave ripples with sinuous crests on upper bedding planes; -Small scale hummocks in sandstones draped by form concordant siltstone or shale lamina; -Centimeter-size load casts; -Small monospecific bivalve molds on upper/lower bedding plane	-Medium-bedding (10–30 cm) -Plane horizontal and current ripple cross-lamination -Load casts -Monospecific bivalve molds on upper/lower bedding plane	-Medium to thick bedding -Tabular, wavy or hummocky shaped sandstone and grainstone beds with internal horizontal or cross-lamination; -Large load casts (ball and pillow structure)	-Very thick bedding; -Evenly bedded/laminated lime mudstones; -Bioclastic/intraclastic detritus accumulated as few cm thick basal lag; -Well preserved fossils; -Gradational transition from lime mudstone to marl; -Intensive bioturbation; -Parallel, slightly undulous or hummocky cross-lamination and grading in calcisiltites; -Gutter casts
Composition	Dolostone: macrocrystalline anhedral to subhedral (Fig. 3) -Primary components: ostracods, ooids/microspheres(?), rare tests of foraminifers Limestone: homogenous crystalline calcite.	Shale–illitic material prevails Siltstone–dominant quartz, less feldspar, varying amount of argillaceous minerals; calcite cement Sandstone–very fine to fine grained, very well sorted quartz arenites/subarcose; rare micaceous rich varieties -Quartz grains dominant; feldspars < 20 %; calcite cement Bioclastic dolostones and calcarenites: consists of microgastropods, bivalves, rare small superficial ooids and/or oncoids and siliciclastic detritus. Oolitic grainstones–dominantly ooids; various amounts of coarse grained to gravel-sized bioclasts (bivalves, microgastropods, echinoderms); small amounts of siliciclastic fine sand sized grains; sparry calcite cement.			Lime mudstone consists of calcite mud; -Bioclasts (mostly echinoid and molluscs) > 2 mm form basal lag; argillaceous component is low. Marl consists of 65 vol.%–75 vol.% of $CaCO_3$, the rest is illitic clay. Occassionaly calcisiltite: skeletal particles (echinoderms or bivalve fragments, foraminifera tests) and silt sized quartz grains; sparry calcite cement
Diagenetic features	-Primary rock structure obliterated by secondary dolomitization -Dedolomitization	-Fe-rich rims of ooids -Macrocrystalline anhedral dolostone structure	-Secondary dolomitization	-Hardground surfaces in oolitic grainstone. -Dolomitization of ooids partial (only nuclei) to complete	Recrystalized calcite mud in lime mudstones
Depositional setting	Coastal part of inner ramp	Inner ramp	Inner ramp	Mid ramp with oolitic shoals	Outer ramp

macrocrystalline anhedral to subhedral (Fig. 4a) and its primary rock structure is obliterated by dolomitization and, occasionally, de-dolomitization processes. Only remnants of ostracods and rare spheroidal forms (ooids/microspheres?) can be observed (Fig. 4a) as well as tests of the foraminifer genus *Earlandia.*

4.2 Siliciclastic Member

Late Griesbachian, Dienerian and Smithian deposits of the Plavno Section (Fig. 2) are represented by interlayered shales, siltstones and sandstones (Figs. 3, 4c–4e) with a thickness of 440 m. The proportion of sandstone/siltstone versus shale beds is variable and is shown in the columnar section (Fig. 3). Intercalation of dolostone, bioclastic and oolitic/oncolitic calcarenite beds rarely occurs. Oolitic grainstones occur in the uppermost part of the Siliciclastic facies (Late Smithian).

Shales consist mainly of illitic material (Aljinović, 1991) while siltstones are composed of quartz, feldspar grains and

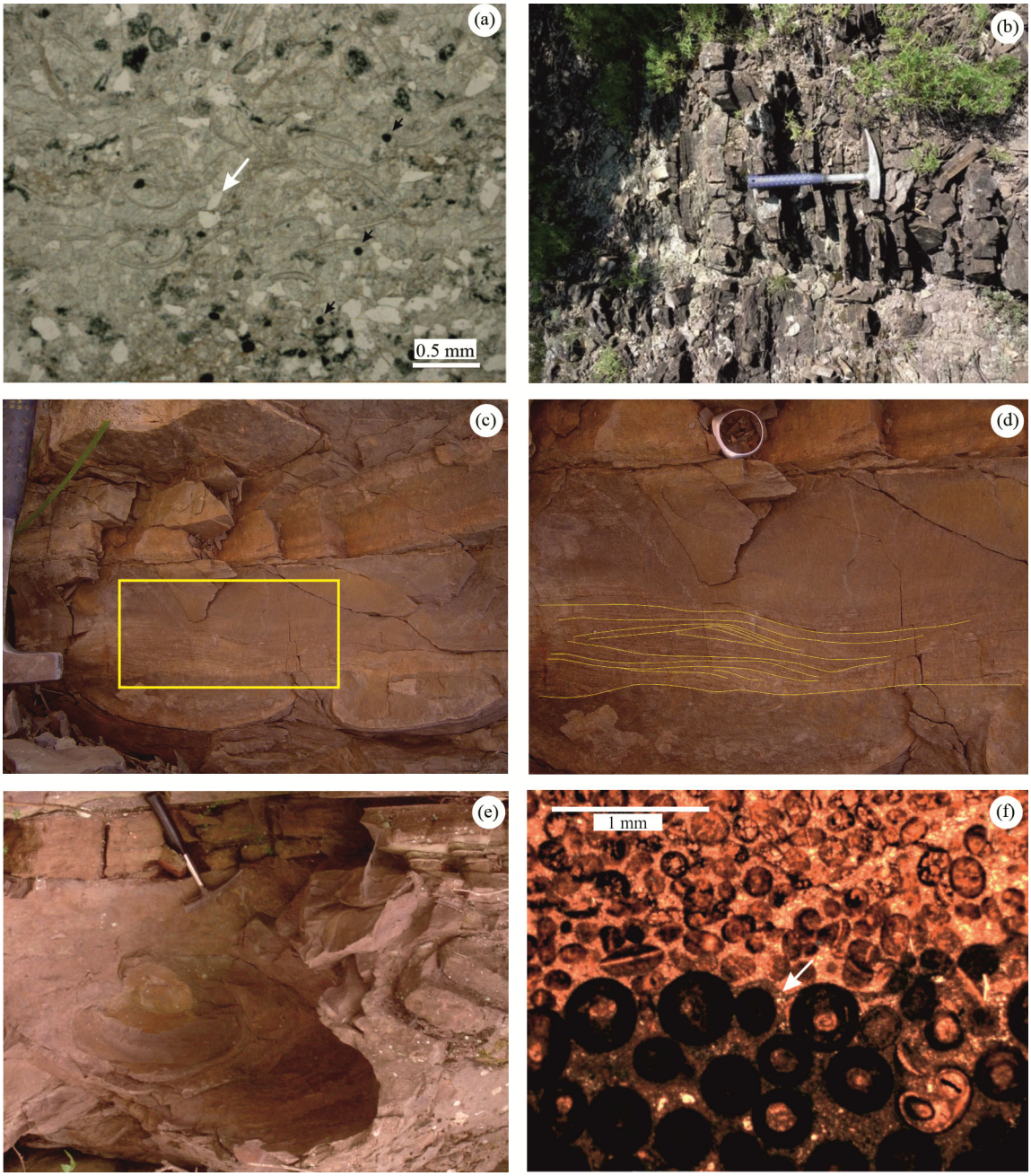

Figure 4. (a) Macrocrystalline structure of late diagenetic dolostone (dolostone member) containing ostracods and siliciclastic grains (arrow); (b) lower interval of the siliciclastic member with grey, even, thinly-bedded (3–10 cm) shale, siltstone and sandstone alternation; vertical beds; stratigraphic top to left; (c) medium thick bedding in the middle interval of the siliciclastic member with load casts often preserved on lower bedding planes; rotated photograph; stratigraphic top is up; (d) enlarged detail from 4c shows a simple internal structure with unidirectional lamina sets overlain by conformable wavy offshooting; rotated photograph; stratigraphic top is up; (e) large load casts in the thick-bedded upper interval of the Siliciclastic member; rotated photograph; stratigraphic top is up; (f) medium sand-sized superficial and radial ooids (upper part of microphotograph) overlay larger, coarse sand-sized tangential ooids (lower part of microphotograph). A firm crust (hardground-arrow) formed between them due to early cementation (Sample Pl-31).

varying amounts of argillaceous minerals and calcite cement (Aljinović, 1991). Sandstones are well-sorted, very fine-grained to fine-grained quartz arenitic to subarcosic types. According to its bed thickness and structural characteristics, the siliciclastic member can be divided into three intervals.

The lower interval consists of grey to yellow, thin shale, siltstone and sandstone beds (Fig. 4b). Horizontal-planar, wavy and current-ripple cross-laminations are common. Sinuous symmetric ripples of wave origin and hummocks are preserved on the upper bedding plane. The lower bedding planes of sandstone and siltstone beds are sharp and often exhibit small load casts or moulds of monospecific bivalves.

In the middle interval, intercalations of red sandstones, siltstones and shales dominate, but with an increasing amount of shale. The thickness of the beds increases from the lower interval (Fig. 4c). Lenticular, wavy or hummocky-shaped beds occur. The most prominent structures in sandstones are horizontal-planar or cross-laminations (sometimes unidirectional ripple cross-lamination) (Fig. 4d), as well as load casts.

The upper interval is characterized by the presence of medium to thick-bedded siliciclastics and oolitic grainstones. Sandstones, siltstones and coarse-grained oolitic grainstones prevail over shale interbeds. The tabular, sometimes wavy or hummocky-shaped sandstone and grainstone beds typically exhibit internal horizontal or cross-lamination. Beds can be deformed due to loading (Fig. 4e).

Grainstones are locally composed of ooids, with significant amounts of coarse-grained to gravel-sized bioclasts (bivalves, microgastropods, echinoderms) and small amounts of siliciclastic sand grains. Varying grain sizes and the cortex fabric suggest different origins of the ooids. Medium sand-sized ooids have characteristics of superficial or radial types, whereas the larger ones (coarse sand-sized) are tangential. In the thick oolite bed marked by Sample Pl-31, two ooid types occur and are separated by a hardground surface (Fig. 4f).

4.3 Mudstone Member

The mudstone member in the Plavno sequence consists of very thick beds of plane-laminated lime mudstones and marls (Fig. 5a). There is an abrupt change from red siliciclastics in the Smithian to grey carbonate-dominated deposition in the Spathian (Figs. 4c, 4d, 4e and 5a–5d for comparison). Ammonoids are exclusively present in this member (listed in Figs. 2 and 3).

Coarse-grained bioclastic or intraclastic detritus, sometimes larger than 2 mm (echinoids and mollusk) is often accumulated as a few-centimeter thick basal lag in mudstone layers (Fig. 5e). Bioturbation is common (Fig. 5b). In the uppermost part of the member, deposition of lime mudstones and marls is frequently accompanied by deposition of 1–20 cm thick laminated calcisiltite layers where basal laminae embrace coarser skeletal particles and are overlain by parallel, slightly undulous (Fig. 5c) or hummocky cross-laminae sets. Well preserved gutter casts are common on the lower bedding planes of the calcisiltites (Fig. 5d). The calcisiltites are composed of skeletal particles and silt-sized quartz grains (Fig. 5f) cemented by sparry calcite.

Deposition does not vary significantly across the Spathian, even at the boundary toward the Anisian.

5 DISCUSSION

5.1 Depositional Model

The Plavno sequence was formed in the so-called Werfen facies belt at the western end of the Tethys Ocean (Scotese et al., 2001) (Fig. 8). The western Tethyan area during the Early Triassic time represented a shallow bay that mostly resembles vast epicontinental sea (Stampfli et al., 2013; Stampfli and Borel, 2002; Scotese, 2001). This long semi-circular palaeogeographic zone stretches several thousand kilometres between Bulgaria in the northeast and the Dinarides in the southwest, and developed as a ramp during the Middle–Late Permian but later evolved into an epeiric shelf during the Early Triassic when the ocean expanded westward (Haas et al., 2007; Hips and Pelikán, 2002; Rüffer and Zühlke 1995; Krainer 1993; Mostler and Rossner 1984). The long-term global sea-level rise (Haq et al., 1987) shifted the coastline toward the west-northwest until the Spathian, when the coastal zone reached the western part of the Northern Calcareous Alps and Southern Alps (Krainer 1993; Broglio Loriga et al., 1990; Mostler and Rossner 1984; Tollmann 1976; Gwinner 1971).

To interpret the vertical facies associations in Plavno, we propose an epeiric ramp model (Fig. 6). Following Burchette and Wright (1992) and Lukasik et al. (2000), we define the epeiric ramp as a homoclinal ramp with a very low bathymetric slope (negligible in its proximal region), a water depth 10s of metres, a width of many hundred kilometres, no distinct shoreface facies, and depositional processes dominated by storms. The epeiric ramp model shares sedimentological characteristics with the epeiric platform (Irwin 1965) and carbonate ramp models (for comparison see Lukasik et al., 2000). In the epeiric ramp, inner, mid- and outer ramp zones can be differentiated (Fig. 6). These zones are divided according to the depth of the fair-weather wave break. From the point the fair-weather waves strike the sea bottom, there exists a narrow high-energy zone with oolitic grainstones. A low energy zone resembling the epeiric platform occurs in the more proximal, shallower part of the ramp. Fair-weather waves dissipate progressively along the inner ramp; therefore, restricting conditions occur in the most inboard facies that were affected primarily by storm and tidal processes and occasionally by waves.

The vertical facies arrangement presented in Fig. 3 is interpreted as a lateral facies shift during long-term transgression (Fig. 6). Deposition in the wide ramp environment seems plausible because metazoan reef builders were generally absent during the Early Triassic (Kiessling, 2010; James, 1984; Flügel, 1982; Heckel, 1974). Ooid-dominated ramps were widespread in periods when framework reefs were globally absent. The abundance of ooids likely reflects low rates of metazoan carbonate production in shallow-water environments, as suggested by Wright and Faulkner (2010) and, Burchette and Wright (1992) and an arid/semi-arid climate (Read, 1998).

In the studied area, the Upper Permian is represented by evaporates deposited in a supratidal (sabkha-like) environment (Tišljar, 1992; Herak, 1973). Casts of halite crystals (Šćavničar, 1973) confirm a shallow hypersaline lagoonal environment. At

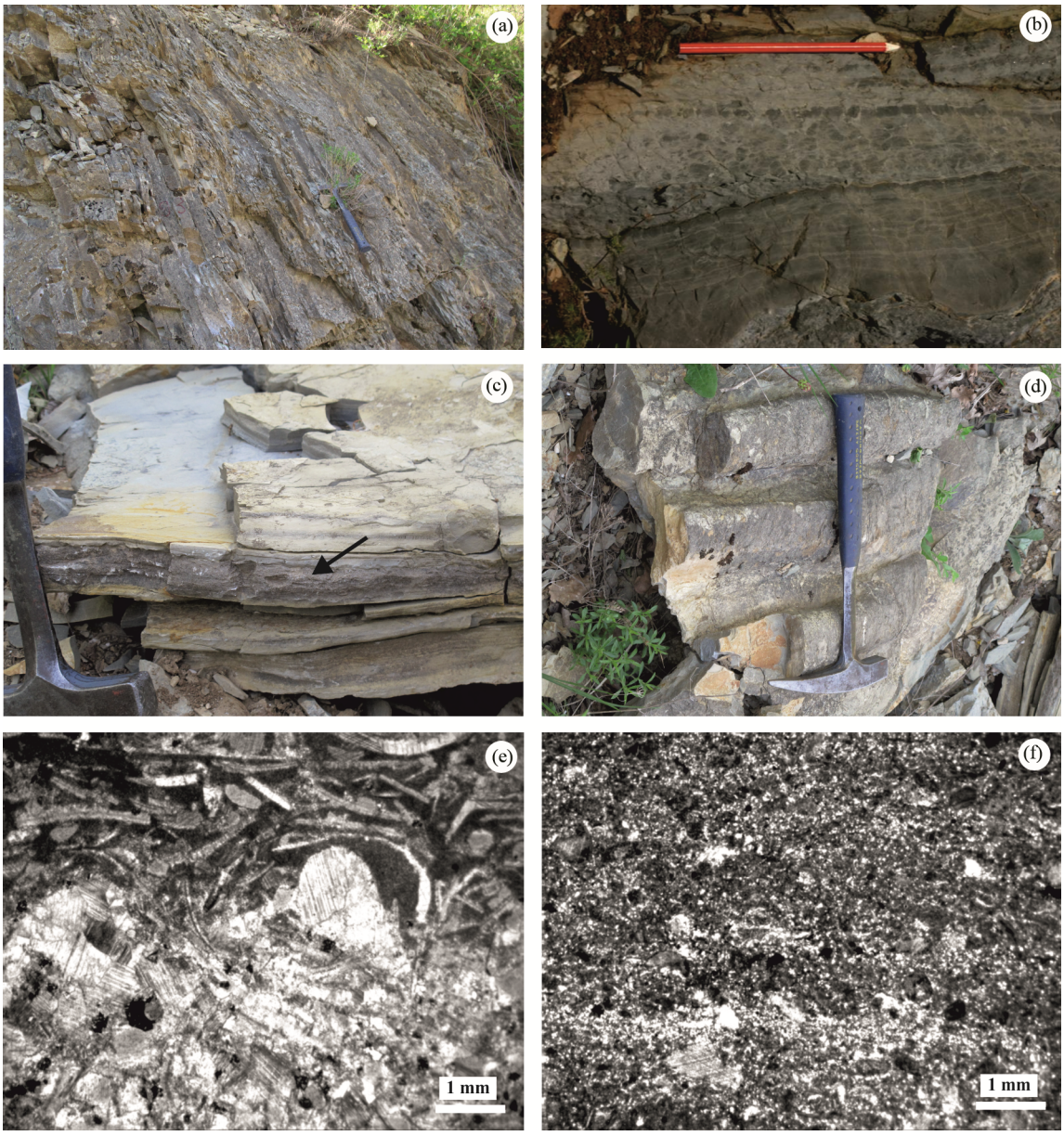

Figure 5. The main lithofacies characterstics of the mudstone member. (a) Evenly bedded/laminated grey lime mudstones. Overturned beds; stratigraphic top to the left. (b) Intense bioturbation in lime mudstones. Vertical position of beds; Photograph is rotated to the right stratigraphic position. (c) Calcisiltite layer—arrow, with a sharp lower bed surface. The amount of silt decreases upward as the mud content increases. (d) Gutter casts on the lower bedding plane of the calcisiltite bed. Vertical bed; Stratigraphic top to left. (e) Microphotograph of coarse-grained bioclastic lag, which accumulated at the base of storm layers in the mudstone member; note an increasing amount of lime mud toward the top. (f) Microphotograph of calcisiltite composed of skeletal particles (usually echinoderms) and silt-sized quartz grains cemented by calcite.

the beginning of the Early Triassic, this supratidal flat/nearshore lagoon developed to an epeiric ramp in the Dinarides.

The EarlyGriesbachian dolostone member of the Plavno sequence likely overlies these Permian evaporates as a conformity, and was deposited after an initial transgression (Tišljar, 1992). The *Hindeodus-Isarcicella* conodont population represents deposition in a shallow subtidal environment, possibly along the inner part of the ramp (Fig. 6). The primary carbonate of the dolostone member underwent severe diagenesis (secondary dolomitization and dedolomitization), complicating the possibility to conduct a detailed sedimentological investigation. Although this dolostone displays features characteristic to burial origin, a primary dolomitization likely occurred before, since Early Triassic primary dolomitic structures are nicely preserved in other parts of the Dinarides (Gorski Kotar, the Velebit Mts., Slovenia). A primary dolostone facies could have occurred in the restricted inner part of the epeiric ramp or on the margin of a lagoon, especially if hypersaline conditions persisted from the Late Permian to the Early Griesbachian (Tucker and Wright, 1990). Dedolomitization is related to the dissolution of underlying evaporites.

Microbial sediments (e.g., stromatolites) that have been reported in many Early Griesbachian sections are missing in Plavno. In the dolostone member microfossils (ostracods,

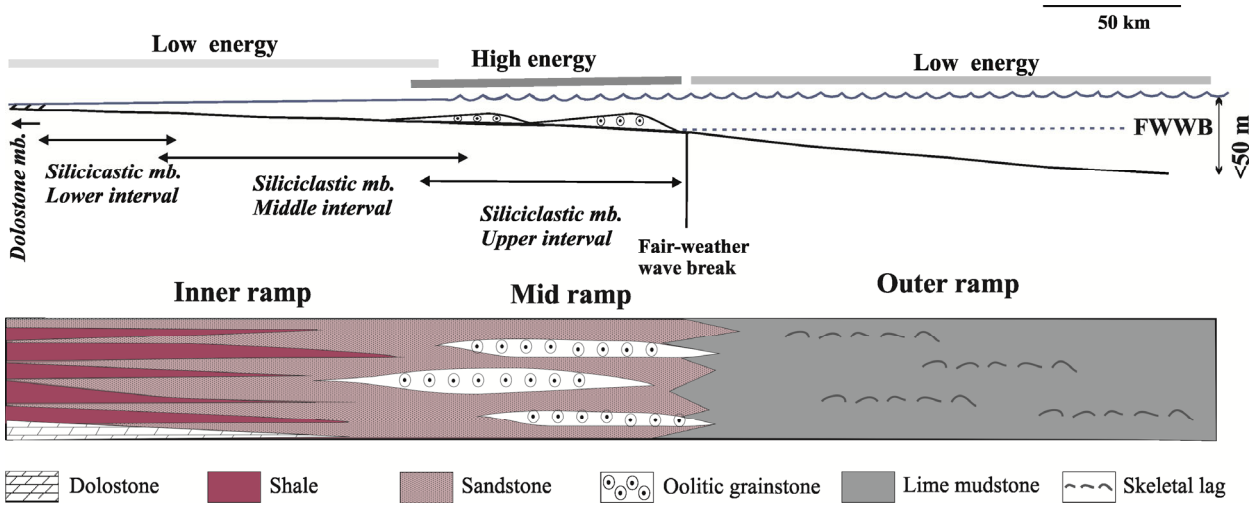

Figure 6. Model of deposition on the epeiric ramp (modified after Lukasik et al., 2000).

foraminifers, conodonts) and macrofossils (bivalves) are rare. The presence of silty/sandy dolostone indicates an intermittently terrigenous influx.

The structural and compositional differences observed in the three intervals of the siliciclastic member are probably controlled by bathymetry and climate. Sedimentation from the dolostone member was transitional and strongly influenced by the deposition of siliciclastic material. Appreciable amounts of feldspar particles in sandstone indicate a preferential mechanical weathering of the uplifted hinterland in arid or semi-arid conditions, as well as enhanced chemical weathering resulting from higher temperatures. Both mechanisms allowed feldspar grains to be preserved (see also Šćavničar and Šušnjara, 1983). The intensity of weathering on land could have been enhanced due to the reduction in vegetation during the end-Permian Extinction (Algeo and Twitchett, 2010; Retallack, 2005, 1995; but see Hochuli et al., 2016). However, as this increase occurred during the uppermost Griesbachian and not directly after the mass-extinction, other mechanisms, such as regional tectonic activity and changes in sea currents, could have played a role. The role of local tectonic activity is further indicated when comparing sedimentation on a regional scale (see Chapter 6.2). Siliciclastic detritus was possibly supplied to the shallow marine environment by short-lived flows that fringed the basin edge and possibly transported alongshore and offshore as in many ancient shallow seas, shelves and ramps (e.g., Johnson and Baldwin, 1996). The appreciable sorting of clastic material stems from transport in alluvial and nearshore zones.

Fine pelitic material was deposited from suspension, whereas horizontal-planar and cross-laminated sandstones and siltstones indicate wave- and current-formed structures. Thin-bedding could have resulted from deposition in a very shallow sub-tidal environment lacking a significant reworking by organisms, like the inner part of the epeiric ramp. The sharp bases of the siltstone and sandstone beds suggest an abrupt commencement of deposition, whereas the vertical grading from sandstone or siltstone to shale indicates deposition under waning energy conditions. Sudden deposition of coarser material over hydroplastic mud caused loading, and could be interpreted as periodic rapid depositional events, such as storms. Other structures, such as the pinch and swell geometry of beds, horizontal planar or ripple cross-lamination, gradation to shale and small-scale hummocks must have been related to waning flows that likely bear witness of storm activity in the shallow part of the epeiric ramp. This is not in accordance with the common occurrence of storm structures in a deeper, transitional zone between the fair-weather and storm-weather wave bases in a shelf/ramp environment (e.g., Aigner, 1985). Storms are capable of reworking the sea floor along the entire epeiric ramp, whereas fair-weather waves affect the sea floor locally. Flat pebbles (fragmentis of shale with plastic deformation accumulated at the base of sandstone beds) can also surve as evidence of *in situ* reworking of the sea floor (Sun et al., 2015; Aljinović et al., 2005). Due to friction along a wide and shallow sea floor, fair-weather waves that impinge the sea bottom in mid ramp (Fig. 6), do not have sufficient strength to rework storm sediments in a nearshore zone (no distinct shoreface facies have been found); therefore, storm deposits can be preserved in the shallow, low-energy environment of the inner epeiric ramp. A considerable amount of siliciclastic mud (shale) has accumulated in the low-energy part of the epeiric ramp. The attenuated bed thickness of the inner epeiric ramp mimics an epeiric "platform".

A similar style of sedimentation (sandstone-siltstone-shale intercalation) persisted in the middle interval, but with an increase in bed thickness. Calcarenites containing bioclasts and ooids occur. The increased bed thickness is interpreted as deposition under the slightly deeper/more distal subtidal conditions of the inner epeiric ramp. Extreme mobility of vast amounts of loose siliciclastic material has to be assumed. Lenticular and hummocky-shaped beds are again evidence of storm origin while shale interlayers represent an overall low energy background deposition during periods without storms.

Abundant casts of bivalve shells preserved in the bedding planes of sandstone/siltstone beds imply instant burial of epifauna under subtidal conditions. Monospecific bivalve fauna and epifaunal activity usually characterize the first stage of ecosystem recovery following the P–T Extinction Event (Twitchett, 2006).

The sandy upper interval of the siliciclastic member also shows evidence of storm deposition. Medium to thick bedding implies more distal position on the epeiric ramp than the previous interval. The prevalence of sandstones and oolitic grainstones in the upper interval suggests high-energy conditions and constant reworking. The origin of the ooids is related to steady, local high-energy conditions in potentially carbonate-rich shoals located away from the shore, where the deposition of siliciclastics was hampered. Formation of ooids could be located in a mid-part of the epeiric ramp, where the fair-weather wave break occurs (Fig. 6). This assumption is supported by the presence of hardgrounds in Bed Pl-31. The formation of hardgrounds in such an environment suggests early cementation due to intensive pumping of water through highly porous sediments (Tucker and Wright, 1990). It is assumed that the sandy material was derived from the nearshore environment, while oolites formed at some distance from shore (Fig. 6). Deposition in the shoals was significantly affected during storms. Storm-driven currents or waves strongly influenced the oolitic shoals, as described by Hine (1977). Nevertheless, storm currents were not able to transport coarse material over long distances in the onshore direction; thus, the ooids stayed restricted within the middle part of the epeiric ramp, while the calcarenites of the middle interval, containing fine and medium grained ooids suggest transport further from the source.

The mudstone member of the Plavno sequence represents a transgressive phase during Spathian time. The presence of ammonoids implies deposition in a slightly deeper environment, namely the outer ramp, and an unrestricted connection with the open sea. Even in this deeper environment, storms exerted a significant influence.

The abundance of fine-grained lime mud and lesser amounts of clay suggest suspension settling in a quiet, low-energy environment and possibly a decrease in weathering on the continent. Gradual deposition of fine-grained carbonate mud was interrupted by deposition periods of coarse skeletal detritus during high-energy events. Layers consisting of coarse well-preserved skeletal and intraclastic lags overlain by lime mud and/or marl are interpreted as distal storm layers. Intense bottom-shear conditions during storm peaks concentrated living and dead shells from the sea bottom, either through burial by storm-suspended particles or through exhuming previously buried shells from underlying weakly-consolidated sediments. Well-preserved fossils and the convex-up position of bivalve and gastropod shells confirm the storm origin because storms tend to bury and protect large/whole fossil fragments from destructive processes (e.g., Kreisa, 1981). The upward fining units consisting of fine-grained sediments deposited from suspension above coarse lag material may also confirm a distal expression of storm activity. No strict structural characteristic could mark the end of a storm and return to normal basin sedimentation, except the intensity of bioturbation.

Deposition of calcisiltites also suggests storm origin. The prevalence of echinoid fragments in the calcisiltites implies transport away from shallower areas, possibly by storms. Calcisiltites represent distal expressions of storm activity and are characterized by weak grading similar to the graded beds described by Reineck and Singh (1972). Hummocky cross-lamination is also evidence of storm activity in a deeper environment far from shore (Kreisa, 1981), whereas gutter casts are attributed to a near bottom storm flow component (Duke, 1990) associated with some helicoidal movements, with axes parallel to the bedding (Whitaker, 1973). According to the elevated sediment tiering in the Plavno sequence, we can conclude that a significant recovery occurred in the Spathian.

The thickness of the Plavno sequence is attributed to a rise in sea level during the Induan accompanied by steady subsidence in this part of the Dinarides. A significant feature of the Plavno epeiric ramp setting is that the entire sea floor was above the storm-weather wave base.

5.2 Comparison of the Plavno Succession with the Western Tethyan Successions of the Werfen Facies Belt

In general, the distribution of carbonate and siliciclastic sediments differs temporally and laterally in the extensive shallow seafloor of the western Tethys. Different successions and transgressive-regressive cycles can be recognized, as summarized in Fig. 7. In this figure, we made correlations based on Plavno's carbon isotope curve using an adapted regional conodont biozonation following Perri (1991), Kolar-Jurkovšek and Jurkovšek (2015), Krystyn et al. (2015) and Chen et al. (2016) and a macrofauna zonation following Golubić (2000) and Posenato (2008). The Early Triassic Plavno sequence reveals similarities and differences to other parts of the Dinarides, as well as sections in the Southern Alps and Hungary (Fig. 7). The palaeogeographic position of Plavno and other important western Tethyan sections is given in Fig. 8. Storm-influenced deposition was recognized as an important mechanism in all sections of the western Tethys. One general trend, however, is the increase of siliciclastics during the Dienerian and Smithian and their replacement by carbonates at the end of the Smithian.

5.2.1 Dinarides

Although there are lithological variations between the different Early Triassic depositional areas in the Dinarides, a general three-fold division is recognizable: the oldest strata consist of carbonates, the middle strata are siliciclastic or mixed carbonate-siliciclastic, and the youngest strata are carbonatic.

5.2.1.1 Gorski Kotar region The Early Triassic sequence of the Gorski Kotar region (~ 190 km northwest of Plavno near the Slovenian border) was interpreted as being deposited on a storm-influenced shelf with oolitic barriers and lagoons that expanded to a broad shallow sea due to transgression (Aljinović et al., 2006). The thick basal oolitic interval (belonging to the *parvus* Zone) was interpreted as an oolitic barrier that was overlain by a dolomitic lagoonal facies (Aljinović et al., 2006). These two facies share many similarities with the Tesero Oolite and Mazzin Member of the Southern and Carnic Alps but do not match facies characteristics the time equivalent dolostone member of the Plavno sequence, which do not reveal distinguishing characteristics of an oolitic barrier. Silici-

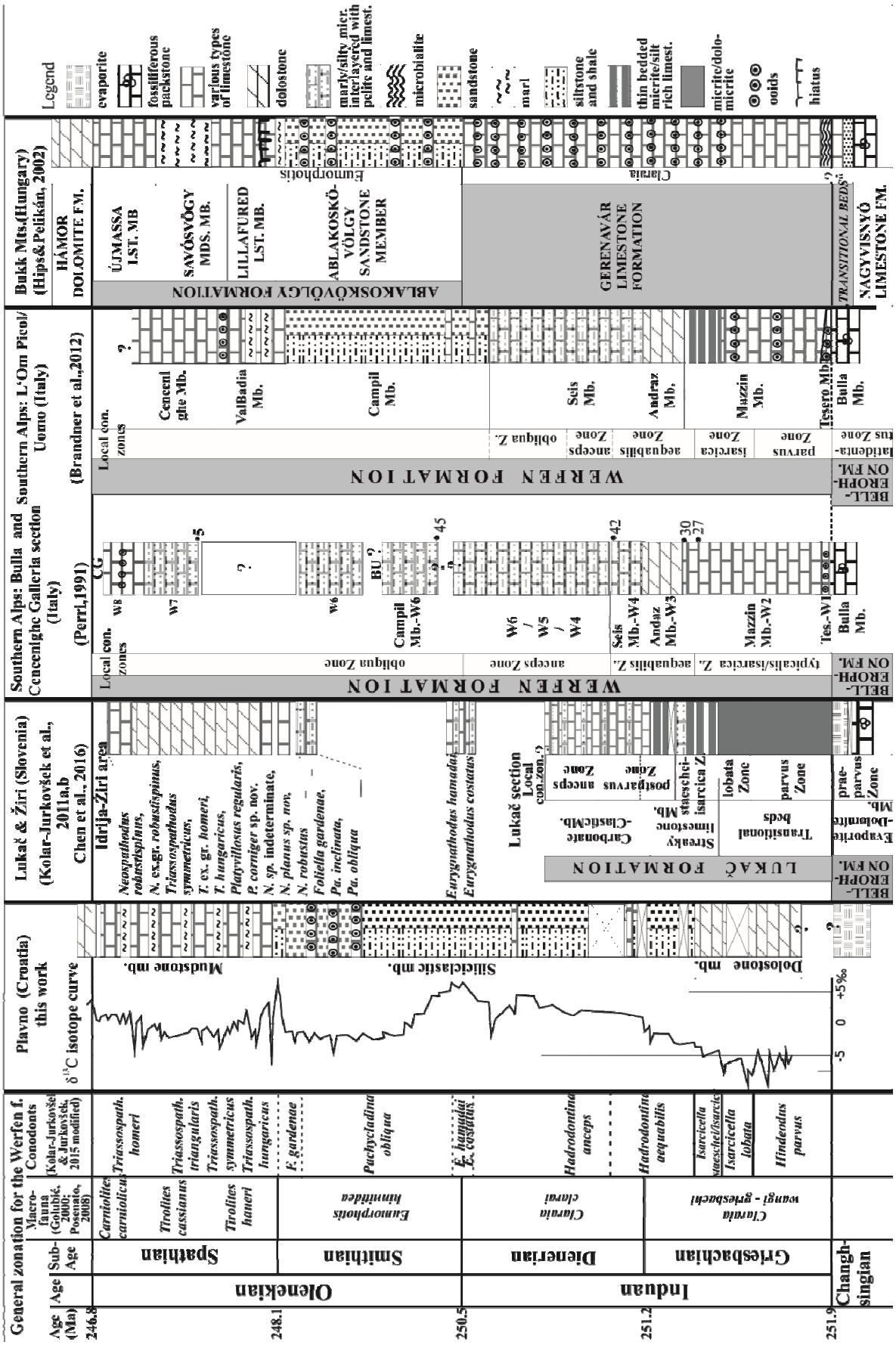

Figure 7. Comparison of the Early Triassic Western Tethyan sections. The lithologic columns are simplified for the sake of comparison. Some lithological terms are used in the original context of the respective authors.

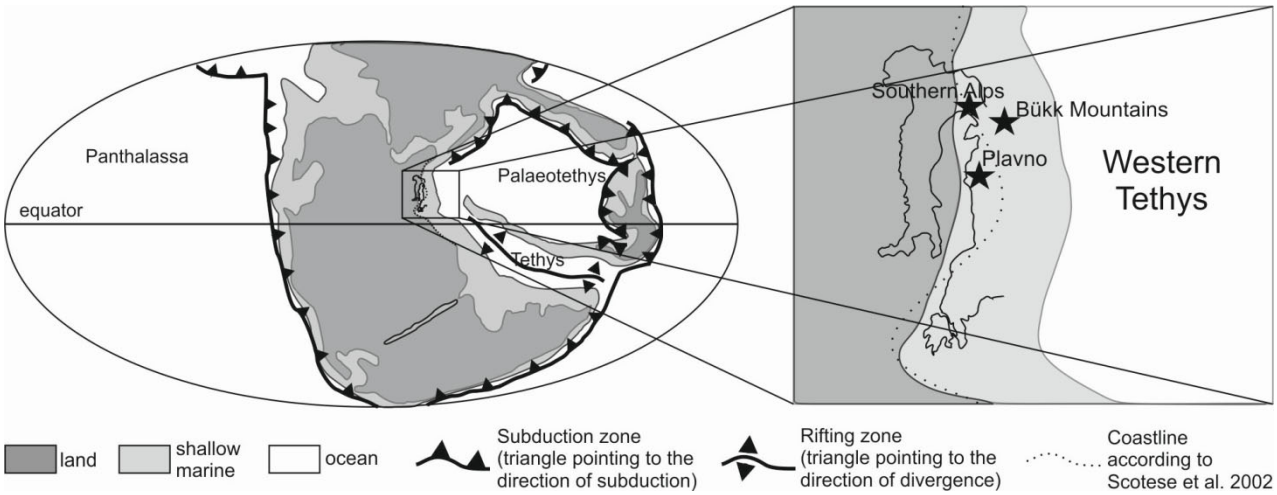

Figure 8. Palaeogeographic reconstruction of the Early Triassic (Scotese et al., 2001) showing the general position of the western Tethys shallow shelf (box). Stars mark supposed positions of the investigated and the most important compared sections.

clastic deposition started later (*Pac. obliqua* Zone) in the Gorski Kotar region than in Plavno (Upper Griesbachian). In Plavno a deposition of siliciclastics started immediately after deposition of the dolostone member and continued until the end of the Smithian, which is consistent with the depositional pattern in Gorski Kotar. Storm currents were important depositional mechanisms in both areas. No distinct facies sharing similarities with the mudstone member were found in the Gorski Kotar region.

5.2.1.2 Lukač and Idrija-Žiri sections (Slovenia) While investigating the Permian and Early Triassic deposits in Slovenia conodont zonation was introduced (summary in Kolar-Jurkovšek and Jurkovšek, 2015) and the following conodont species were distinguished: *Hindeodus praeparvus* Z., *H. parvus* Z., *Isarcicella lobata* Z., *I. staeschei-I. isarcica* Z., *H. postparvus* Z., *Hadrodontina aequabilis* Z., *Ha. anceps* Z., *Eurygnathodus costatus* Z., *Neospathodus planus* Z., *N. robustus* Z., *Platyvillosus corniger* Z., *Pl. regularis* Z., *Pachycladina obliqua* Z., *Foliella gardeane* Z., *Triassospathodus hungaricus* Z., *T. symmetricus* Z., *N. robustispinus-T. homeri* Z. and *T. triangularis* Z.. Certain levels of the Early Triassic succession in Slovenia are marked by shallow water genera and the introduced conodont zonation is valid for shallow shelf environments of the western Tethys (Kolar-Jurkovšek and Jurkovšek, 2015, see references therein).

Among the several investigated sections, the PTB was defined in Slovenia only in the Lukač Section near Žiri in the External Dinarides, according to an international criterion based on the finding of the conodont species *H. parvus* (Kolar-Jurkovšek et al., 2016, 2011a, b; Kolar-Jurkovšek and Jurkovšek, 2015, 2007).

The following similarities/differences can be observed in the Slovenian part of the External Dinarides (Lukač and Idrija-Žiri sections, Kolar-Jurkovšek et al., 20011a, b; Nestell et al., 2011). Like Plavno, the dolostone of the Lukač Section overlies thick evaporitic deposits. In the Lukač Section, the evaporite-dolomite member (Mb.), representing the topmost part of the Upper Permian Bellerophon Formation, is overlain by Transitional beds (where the PT boundary was identified), and the Streaky limestone Mb. Transitional beds (laminated mudstones, biomicrites rich in ostracods and dolomitized oolitic grainstones) of the Griesbachian *parvus*-, *lobata*- and *staeschei-isarcica* Zones were deposited in shallow relatively restricted subtidal marine conditions. The time equivalent of the Transitional beds is the dolostone Mb. of the Plavno Section (*parvus-isarcica* Zone). The scarce presence of ostracods and ooids/microspheres(?) suggests their lithological and environmental similarity. The Streaky limestone Mb. shares some similarities with the lower interval of the siliciclastic Mb. as both facies are characterized by thin-bedding and storm structures. However, in the Plavno sequence, this interval is almost purely siliciclastic, in comparison to the Lukač Section which is dominantly calcareous. In the Lukač Section, the Streaky limestone Mb. is followed by the carbonate-clastic Mb. of the Late Griesbachian and Early Dienerian (*postparvus* and *anceps* conodont Zones). It consists of increasing amounts of siliciclastics, but with substantial limestone presence (oolitic grainstones and micrites/biomicrites). These deposits mirror a very shallow depositional environment due to oscillatory currents (Kolar-Jurkovšek et al., 2011a). The time equivalent middle interval of the siliciclastic member of the Plavno sequence contains comparatively more siliciclastic material.

The Idrija-Žiri sequence of Slovenia can be seen as a stratigraphic continuation of the Lukač Section since it starts stratigraphically above the later—around the DSB—and ends in the Late Spathian (Chen et al., 2016). From the very beginning the Idrija-Žiri sequence is quite calcareous and the Smithian interval is thus more similar to the Southern Alps than to Plavno. During the Spathian, Žiri shows widespread dolomitization that makes detailed facial comparisons difficult. Astonishing is, however, the rich conodont representation which points to a more open-marine and more distal shelf position than all described sections including Plavno.

Recent reports from Serbia (Sudar et al., 2014, 2007; Nestell et al., 2009) from an exotic block terrane within the Vardar Zone (Inner Dinarides) are not dealt with here as they mostly include palaeontological data or refer exclusively to the

Permian-Triassic boundary interval.

5.2.2 Transdanubia and Bükk Mountains (Hungary)

In the Early Triassic sequences from Hungary, the Permian-Triassic boundary interval (investigated in the core sections of the Transdanubian Range) represent an inner ramp setting where oolitic facies overlie lagoonal-sabkha deposits, with some resemblance to the basal part of the Plavno sequence (Haas et al., 2007, 2004).

The Early Triassic sequence investigated in the Bükk Mountains (Hips and Pelikán, 2002) (Fig. 7), was deposited on the epeiric shelf of the western Tethys. The Bükk sequence (Hips and Pelikán, 2002) consists of two formations: the Grennavár limestone formation (Upper Changshsingian–Griesbachian) and the Ablakoskovölgy Formation (Dienerian–Spathian, divided into the Ablakoskovölgy sandstone, Lillafured limestone), Savósvölgy marl and Újmassa limestone members. In the Bükk sedimentary sequence, transgressive-regressive cycles have been observed (Hips and Pelikán, 2002), whereas the Plavno represents a long-term transgressive sequence. On the contrary, Hips and Pelikán (2002) concluded that local subsidence plays an important role in establishing several short term transgressive-regressive trends.

In its lower interval (*parvus* and *isarcica* conodont Zones), the Gerennavár limestone formation reflects deposition of peritidal microbial and finely laminated mudstones and mudstone-wackestones of a shallow subtidal lagoon (Hips and Pelikán, 2002) or an outer ramp (Haas et al., 2007, 2004). Microbial facies is missing in the time equivalent interval of the Plavno Section. The upper part of the Gerennavár limestone formation, which is composed of thick-bedded oolites and bioclastic grainstones of Late Griesbachian and Early Dienerian ages, has no facial equivalent in the Plavno sequence. It was deposited in a high-energy tide and wave-dominated shallow shelf characterized as a protected, stabilized muddy sand flat and a high-energy sand belt. The time equivalent lower interval of the siliciclastic member deposited in Plavno reflects sedimentation on a low-energy proximal ramp. Several more similarities in depositional characteristics occur between the Ablakoskovölgy sandstone Mb. and the middle and upper siliciclastic member of the Plavno sequence. It is obvious that siliciclastic influx intensified in both sections during the Dienerian and Smithian. The siliciclastic rich, lower part of the Ablakoskovölgy Formation indicates a mixed, dominantly siliciclastic shallow shelf, with deposition in the coastal, shoreface and transitional zones (Hips and Pelikán, 2002). The carbonates deposited in the upper part of the Ablakoskovölgy Formation indicate a storm-controlled shelf, with facies of the peritidal-shallow shoals to the low-energy deeper subtidal zone below the storm wave-base. In the Plavno Section, the middle and upper intervals of the Siliciclastic Mb. show similar lithology (siliciclastic-oolitic grainstone intercalation) with the Ablakoskovölgy sandstone Mb. having been deposited in the distal part of the epeiric ramp, partly in the high-energy zone around the fair-weather wave base due to persistent transgression. Deposition was influenced by storms in both sections. The prevalence of carbonates in the Lillafured limestone Mb., Savósvölgy marl Mb. and Újmassa limestone Mb. (Spathian) were interpreted as being deposited in storm-dominated peritidal shoals to low-energy deeper subtidal zones below the storm wave base (regressive-transgressive cycle, Hips and Pálikán, 2002). This differs from the deposition of the mudstone Mb. of Plavno deposited in the distal part of the epeiric ramp, but above storm-wave base.

5.2.3 Southern Alps

The Early Triassic sequences of the Dinarides were traditionally correlated with the Werfen Formation in the Southern Alps, but it seems that the studied sections (Plavno, Bulla), Cencenighe Galleria, L'Omo Picol (all belonging to western Tethyan depositional area) reveal significant differences (Fig. 7). Storms were recognized as an important depositional mechanism in both areas. At least four transgressive-regressive cycles were documented in the Early Triassic Southern Alpine sections (Brandner et al., 2012, 2009), whereas in the Plavno sequence it is interpreted as one long-term transgressive cycle. In the well-known localities in the Southern Alps at Bulla and Tesero, several members were lithostratigraphically, biostratigraphically and sedimentologically differentiated (Brandner et al., 2012, 2009; Perri and Farabegoli, 2003; Farabegoli and Perri, 1998; Perri, 1991; Perri and Andraghetti, 1987, and references therein). The Tesoro Mb. at the base of the Werfen Formation is characterized by various thick layers of oolitic grainstones and was interpreted as a shoreface or oolitic bar facies (Brandner et al., 2012; Perri and Farabegoli, 2003) gradually passing upwards into the Mazzin Mb. (grey mudstone, sometimes microbial) deposited in the mid or outer ramp position below the wave base. Despite the time correspondence, petrographical characteristics of the dolostone Mb. of the Plavno sequence do not provide sufficient evidence to be identified either with the Tesero or the Mazzin Mb. because late dolomitization destroyed the primary sedimentary features. Only rare occurrences of calcitic microspheres (resembling ooids) are common to both regions. Mudstones and microbial mudstones of the Mazzin Mb. are also absent as well as the tidal flat dolomites of the Andraz Horizon due to an earlier onset of siliciclastic sedimentation in Plavno.

The carbonate-dominated Seis Mb. of the Dienerian differs from the intensive siliciclastic regime in the time equivalent of the Plavno Section. Only the storm deposits of the Gastropod oolite facies in the Upper Seis Member demonstrate similar conditions in both regions with respect to storm influence. The Spathian Val Badia and Cencenighe Mbs. are interpreted as storm-influenced deposits with varying siliciclastic input. Both members compare well with the mudstone Mb. of the Plavno sequence, however, they represent more proximal and shallower depositional settings. Described differences possibly stem from local controls on deposition (e.g., the amount of siliciclastic input, proximity of land as a clastic source area), antecedent topography and characteristics of depositional environment.

6 CONCLUSIONS

The Early Triassic ~1 000 m thick Plavno succession was investigated by litho-, bio- and chemostratigraphic methods. A continuous ^{13}C isotope curve was obtained. The isotope data

combined with the analysis of conodonts, bivalves and ammonoids served to establish Early Triassic substage boundaries for the first time in the Dinarides.

Lithostratigraphically, the Plavno sequence was divided into three informal units: (1) the dolostone member (Early Griesbachian); (2) the siliciclastic member, further divided into lower, middle and upper intervals (Late Griesbachian, Dienerian and Smithian, respectively); and (3) the mudstone member (lime mudstones, marls and calcisiltites with common ammonoids and gastropods—Spathian). The initial transgression at the beginning of the Early Triassic resulted in flooding of the Permian evaporitic basement and the continuous deposition on the epeiric ramp reflecting a long-term transgression. The Plavno sequence is characterized by storm-dominated deposition on a very low bathymetric ramp slope (epeiric ramp). The entire deposition occurred above the storm-weather wave base, in a relatively shallow water (approx. 10s of metres depth). Deposition of the dolostone member (Early Griesbachian) and the lower interval of siliciclastic member (Upper Griesbachian) occurred in the low energy inner ramp zone that was storming influenced (Fig. 6). From the end of the dolostone member to the base of the siliciclastic member, deposition of siliciclastics dramatically increased and dominated from the Upper Griesbachian to the end-Smithian. The continuous transgression resulted in the sedimentation of the middle interval deposits of the siliciclastic member in a slightly deeper part of the low-energy inner ramp. Sandy-oolitic deposits in the upper interval of the siliciclastic member (Smithian) were deposited in the high-energy mid ramp. The formation of ooids was possible only in the high-energy area around the fair-weather wave base. Below the fair-weather wave base, in the low-energy outer ramp the deposition of lime muds, marls and ammonoid-bearing tempestite beds prevail (Fig. 6). These conditions were established at the beginning of the Spathian when the mudstone member was deposited. This could be the result of the known global transgression during the Spathian. Episodic storms were able to rework the sea floor along the entire epeiric ramp, while fair-weather waves affected the sea floor locally.

Comparison of Plavno with other western Tethyan depositional areas demonstrates differences specifically in Dienerian and Smithian time where the high siliciclastic content likely stems from local controls on deposition within this large shallow marine environment. The greatest similarities can be observed with the Bükk Mts. sequence which is in accordance with the palaeogeographic reconstruction by Haas et al. (1995) who placed the Bükk Mts. adjacent to the NW Dinarides.

ACKNOWLEDGMENTS

The field data were obtained during 2012. The investigation was part of the Austrian-Croatian Bilateral Project (No. 2014-15) supported by OeAD; the Austrian Agency for International Mobility and Cooperation in Education; and the Croatian Ministry of Science, Education and Sport. This research was partly supported by the Slovenian Research Agency (No. P1-0011). The facilities of the Geological Survey of Slovenia are acknowledged. This article is a contribution to IGCP 572 and IGCP 630. We would like to thank F Read and Y D Sun for their constructive comments which significantly helped to improve this contribution. We are especially grateful to Miss Lauren Chen for her help in language editing. The final publication is available at Springer via https://doi.org/10.1007/s12583-018-0787-3.

Electronic Supplementary Materials: Supplementary materials are available in the online version of this article at https://doi.org/10.1007/s12583-018-0787-3.

REFERENCES CITED

Aigner, T., 1985. Storm Depositional Systems: Dynamic Stratigraphy in Modern and Ancient Shallow-Marine Sequences. Lecture Notes in Earth Sci., 3, Springer-Verlag, New York. 173

Algeo, T. J., Twitchett, R. J., 2010. Anomalous Early Triassic Sediment Fluxes due to Elevated Weathering Rates and Their Biological Consequences. *Geology*, 38(11): 1023–1026. https://doi.org/10.1130/g31203.1

Aljinović, D., 1991. Petrographic and Sedimentologic Characteristics of the Early Triassic Deposits in the Plavno and Strmica: [Dissertation]. University of Zagreb, Zagreb. 92

Aljinović, D., 1995. Storm Influenced Shelf Sedimentation—An Example from the Lower Triassic (Scythian) Siliciclastic and Carbonate Succession near Knin (Southern Croatia and Western Bosnia and Herzegovina). *Geologia Croatica*, 48: 17–32

Aljinović, D., 1997. Facijesi Klasičnih Sedimenata Mlađeg Paleozoika i Starijeg Trijasa Gorskog Kotara (Late Palaeozoic and Early Scythian Clastic Facies in Gorski Kotar, Croatia): [Dissertation]. University of Zagreb, Zagreb. 163

Aljinović, D., Kolar-Jurkovšek, T., Jurkovšek, B., 2005. Litofaciesna in Konodontna Conacija Spodnjetriasnih Plasti Severozahodnega Dela Zunanjih Dinaridov (Gorkski Kotar, Hrvaška). *RMZ-Materials and geoenvironment RMZ-materiali in geookolje*, 52: 581–596

Aljinović, D., Kolar-Jurkovšek, T., Jurkovšek, B., 2006. The Lower Triassic Shallow Marine Succession in Gorski Kotar Region (External Dinarides, Croatia): Lithofacies and Conodont Dating. *Rivista Italiana di Paleontologia e Stratigrafia*, 112: 35–53

Aljinović, D., Kolar-Jurkovšek, T., Jurkovšek, B., et al., 2011. Conodont Dating of the Lower Triassic Sedimentary Rocks in the External Dinarides (Croatia and Bosnia and Herzegovina). *Rivista Italiana di Paleontologia e Stratigrafia*, 117: 135–148

Assereto, R., Bosellini, A., Fantini Sestini, N., et al., 1973. The Permian-Triassic Boundary in the Southern Alps (Italy). In: Logan, A., Hills, L. V., eds., The Permian and Triassic Systems and Their Mutual Boundary. *Canadian Soc. Petroleum Geol. Mem*., 2: 176–199

Babić, L. J., 1968. O Trijasu Gorskog Kotara i Susjednih Područja (Sur le Trias Dans le Gorski Kotar et les Regions Voisines). *Geol. Vjesnik*, 22: 11–23

Bauer, F. K., Cerny, I., Exner, C., et al., 1983. Erlauterungen zur Geologischen Karte der Karawanken 1 : 25 000. Geologische Bundesanstalt Wien, Ostteil. 86

Bosellini, A., 1964. Stratigrafia, Petrografia e Sedimentologia Delle Facies Carbonatiche al Limite Permiano-Trias Nelle Dolomiti Occidentali. *Mem. Mus. St. Nat. Ven. Trid.*, 15: 59–110

Bosellini, A., 1968. Paleogeologia Pre-Anisica Delle Dolomiti Centrosettentrionali. *Atti Accademia Nazionale dei Lincei. Memorie della Classe di Scienza Fisiche Matematiche e Maturali*, 9(8): 1–33

Brandner, R., Horacek, M., Keim, L., et al., 2009. The Pufels/Bulla Road

Section: Deciphering Environmental Changes across the Permian-Triassic Boundary to the Olenekian by Integrated Litho-, Magneto- and Isotope Stratigraphy: A Field Trip Guide. *Geo. Alp*., 6: 116–132

Brandner, R., Horacek, M., Keim, L., 2012. Permian-Triassic-Boundary and Lower Triassic in the Dolomites, Southern Alps (Italy). Field Trip Guide 29th IAS Meeting of Sedimentology Schladming/Austria. *Journal of Alpine Geology*, 54: 379–404

Broglio Loriga, C., Masetti, D., Neri, C., 1983. La formazione di Werfen (Scitico) Delle Dolomiti Occidental: Sedimentologia e Biostratigrafia. *Riv. Ital. Paleont. Strat.*, 88: 501–598

Broglio Loriga, C., Neri, C., Posenato, R., 1986. The Lower Triassic of the Dolomites and Cadore. In: Italian IGCP 203 Group, Permian and Permian-Triassic Boundary in the South-Alpine Segment of the Western Tethys: Field-Guide Book. Soc. Geol. It. and IGCP 203 Meeting, July 4–12, 1986, Brescia. 29–34

Broglio Loriga, C., Góczán, F., Haas, J., et al., 1990. The Lower Triassic Sequence of the Dolomites (Italy) and Transdanubian Mid-Mountains (Hungary) and Their Correlation. *Memorie di Scienze Geologiche*, 42: 41–103

Burchette, T. P., Wright, V. P., 1992. Carbonate Ramp Depositional Systems. *Sedimentary Geology*, 79(1/2/3/4): 3–57. https://doi.org/10.1016/0037-0738(92)90003-a

Chen, Y. L., Kolar-Jurkovšek, T., Jurkovšek, B., et al., 2016. Early Triassic Conodonts and Carbonate Carbon Isotope Record of the Idrija–Žiri Area, Slovenia. *Palaeogeography*, *Palaeoclimatology*, *Palaeoecology*, 444: 84–100. https://doi.org/10.1016/j.palaeo.2015.12.013

Chorowitz, J., 1977. Etude Geologique des Dinarides le Long de la Structure Transverale Split-Karlovac (Yugoslavie). *Societé Gêologique du Nord*, 1: 3–331

Clarkson, M. O., Richoz, S., Wood, R. A., et al., 2013. A New High-Resolution $\delta^{13}C$ Record for the Early Triassic: Insights from the Arabian Platform. *Gondwana Research*, 24(1): 233–242. https://doi.org/10.1016/j.gr.2012.10.002

De Zanche, V., Farabegoli, E., Mietto, P., et al., 1980. Le Unità Litostratigrafiche al Limite Scitico-Anisico nel Recoarese (Prealpi Vicente). *Mem. Sci. Geol.*, 34: 195–204

De Zanche, V., Gianolla, P., Mietto, P., et al., 1993. Triassic Sequence Stratigraphy in the Dolomites (Italy). *Mem. Sci. Geol.*, 45: 1–27

Duke, W. L., 1990. Geostrophic Circulation or Shallow Marine Turbidity Currents? the Dilemma of Paleoflow Patterns in Strom-Influenced Prograding Shoreline Systems. *Journal of Sedimentary Research*, 60(6): 870–883. https://doi.org/10.1306/d4267636-2b26-11d7-8648000102c1865d

Đurđanović, Ž., 1967. The Lower Triassic of the Gorski Kotar Region. *Geol. Vjesnik*, 20: 107–110

Farabegoli, E., Perri, M. C., 1998. Permian/Triassic Boundary and Early Triassic of the Bulla Section (Southern Alps, Italy): Lithostratigraphy, Facies and Conodont Biostratigraphy. In: Perri, M. C., Spalletta, C., eds., Southern Alps Field Trip Guidebook. *ECOS VII. Giornale di Geologia* (*Spec. Issue*), 60: 292–310

Flügel, E., 1982. Evolution of Triassic Reefs: Current Concepts and Problems. *Facies*, 6(1): 297–327. https://doi.org/10.1007/bf02536687

Goldring, R., Bridges, P., 1973. Sublitoral Sand Sheets. *Jour. Sed. Petrology*, 43: 736–747

Golubić, V., 2000. Biostratigraphic Distribution of Upper Scythian Ammonites in the Reference Area of Muć Gornji Village, Croatia. *Natura Croatica*, 9: 237–274

Grasby, S. E., Beauchamp, B., Embry, A., et al., 2012. Recurrent Early Triassic Ocean Anoxia. *Geology*, 41(2): 175–178. https://doi.org/10.1130/g33599.1

Grimani, I., Šikić, K., Šimunić, A., 1972. Osnovna Geološka Karta SFRJ, 1 : 100 000, List Knin. (Basic Geologic Map SFRJ). Institut za Geološka Istraživanja Zagreb, Savezni Geol. Zavod Beograd.

Grimani, I., Šikić, K., Šimunić, A., 1975. Osnovna Geološka Karta SFRJ, 1 : 100 000, Tumač za List Knin (Basic Geologic Map SFRJ Explanatory Notes to Geological Map—Knin; Abs: Geology of the Knin Sheet). Institut za Geološka Istraživanja Zagreb, Savezni Geol. Zavod Beograd. 61

Gwinner, M. P., 1971. Geologie der Alpen—Stratigraphie, Pläogeographie, Tektonik. Schweizerbartsche Verlagsbuchhandlung, Stuttgart. 477

Haas, J., Kovács, S., Krystyn, L., et al., 1995. Significance of Late Permian-Triassic Facies Zones in Terrane Reconstructions in the Alpine-North Pannonian Domain. *Tectonophysics*, 242(1/2): 19–40. https://doi.org/10.1016/0040-1951(94)00157-5

Haas, J., Hips, K., Pelikán, P., et al., 2004. Facies Analysis of Marine Permian/Triassic Boundary Sections in Hungary. *Acta Geologica Hungarica*, 47(4): 297–340. https://doi.org/10.1556/ageol.47.2004.4.1

Haas, J., Demény, A., Hips, K., et al., 2007. Biotic and Environmental Changes in the Permian-Triassic Boundary Interval Recorded on a Western Tethyan Ramp in the Bükk Mountains, Hungary. *Global and Planetary Change*, 55(1/2/3): 136–154. https://doi.org/10.1016/j.gloplacha.2006.06.010

Haq, B. U., Hardenbol, J., Vail, P. R., 1987. Chronology of Fluctuating Sea Levels since the Triassic. *Science*, 235(4793): 1156–1167. https://doi.org/10.1126/science.235.4793.1156

Heckel, P. H., 1974. Carbonate Buildups in the Geological Record: A Review. In: Laporte, L. F., ed., Reef in Time and Space. *Soc. Econ. Paleontol. Mineral.* (*Spec. Publ.*), 18: 90–154

Herak, M., 1973. Some Teclonical Problems of the Evaporitic Area in the Dinarides of Croatia. *Geol. Vjesnik*, 26: 29–40

Herak, M. 1986. A New Concept of Geotectonics of the Dinarides. *Acta Geologica*, 16(1): 1–42

Herak, M., Šćavničar, B., Šušnjara, A., et al., 1983. Neue Beiträge zur Biostratigraphie der Tethys-Trias. Lower Triassic of Muć. Proposal for standard section of the European Upper Scythian. *Schr. Erdwiss*., 5, 93-106.

Hine, C. A., 1977. Lily Bank, Bahamas: History of an Active Oolite Sand Shoal. *SEPM Journal of Sedimentary Research*, 47: 1554–1583.

Hips, K., Pálikán, P., 2002. Lower Triassic Shallow Marine Succession in the Bükk Mountains, NE Hungary. *Geol. Carpathica*, 53(6): 351–367

Hochuli, P. A., 2016. Interpretation of "Fungal Spikes" in Permian-Triassic Boundary Sections. *Global and Planetary Change*, 144: 48–50. https://doi.org/10.1016/j.gloplacha.2016.05.002

Horacek, M., Brandner, R., Abart, R., 2007a. Carbon Isotope Record of the P/T Boundary and the Lower Triassic in the Southern Alps: Evidence for Rapid Changes in Storage of Organic Carbon. *Palaeogeography*, *Palaeoclimatology*, *Palaeoecology*, 252(1/2): 347–354. https://doi.org/10.1016/j.palaeo.2006.11.049

Horacek, M., Richoz, S., Brandner, R., et al., 2007b. Evidence for Recurrent Changes in Lower Triassic Oceanic Circulation of the Tethys: The $\delta^{13}C$ Record from Marine Sections in Iran. *Palaeogeography*, *Palaeoclimatology*, *Palaeoecology*, 252(1/2): 355–369. https://doi.org/10.1016/j.palaeo.2006.11.052

Horacek, M., Koike, T., Richoz, S., 2009. Lower Triassic $\delta^{13}C$ Isotope Curve from Shallow-Marine Carbonates in Japan, Panthalassa Realm: Confirmation of the Tethys $\delta^{13}C$ Curve. *Journal of Asian Earth*

Sciences, 36(6): 481–490. https://doi.org/10.1016/j.jseaes.2008.05.005

Horacek, M., Povoden, E., Richoz, S., et al., 2010. High-Resolution Carbon Isotope Changes, Litho- and Magnetostratigraphy across Permian-Triassic Boundary Sections in the Dolomites, N-Italy. New Constraints for Global Correlation. *Palaeogeography*, *Palaeoclimatology*, *Palaeoecology*, 290(1/2/3/4): 58–64. https://doi.org/10.1016/j.palaeo.2010.01.007

Horacek, M., Krystyn, L., Brandner, R., 2015. Significance of Platyvilosus Costatus and Foliella Gardenae as Indicators for the Dienerian-Smithian and Smithian-Spathian Boundaries, Respectively: A Study in the Dolomites (N-Italy). EGU General Assembly 2015, April 12–17, 2015, in Vienna, Austria. *Geophysical Research Abstracts*, 17: EGU2015-14921

Irwin, M. L., 1965. General Theory of Epeiric Clear Water Sedimentation. *AAPG Bulletin*, 49: 445–459

Ivanović, A., Šćavničar, B., Sakač, K., et al., 1971. Stratigrafski Položaj i Petrografske Karakteristike Evaporita i klastita Okolice Drniša i Vrlike u Dalmaciji (Stratigraphic Possition and Petrographical Characteristics of the Evaporite and Clastic Deposits in the Environs of Drniš and Vrlika (Dalmatia)). *Geol. Vjesnik*, 24: 11–33

Ivanović, A., Sikirica, V., Sakač, K., 1978. Osnovna Geološka Karta 1 : 100 000, Tumač za List Drniš K33-9 (Explanatory Notes to Geological Map-Drniš). Institut za Geološka Istraživanja Zagreb, Savezni Geol. Zavod Beograd

James, N. P., 1984. Reefs. In: Walker, R. G., ed., Facies Models. *Geosci. Canad. Repr. Ser.*, 1: 229–244

Jelaska, V., Kolar-Jurkovšek, T., Jurkovšek, B., et al., 2003. Triassic Beds in the Basement of the Adriatic-Dinaric Carbonate Platform of the Svilaja Mt. (Croatia). *Geologija*, 46(2): 225–230. https://doi.org/10.5474/geologija.2003.019

Johnson, H. D., Baldwin, C. T., 1996. Shallow Clastic Seas. In: Reading, H. G., ed., Sedimentary Environments: Processes, Facies and Stratigraphy, 3rd Edition. Blackwell Science Ltd., Oxford. 232–281

Kiessling, W., 2010. Reef Expansion during the Triassic: Spread of Photosymbiosis Balancing Climatic Cooling. *Palaeogeography*, *Palaeoclimatology*, *Palaeoecology*, 290(1/2/3/4): 11–19. https://doi.org/10.1016/j.palaeo.2009.03.020

Kolar-Jurkovšek, T., Jurkovšek, B., 2007. First Record of Hindeodus–Isarcicella Population in Lower Triassic of Slovenia. *Palaeogeography*, *Palaeoclimatology*, *Palaeoecology*, 252(1/2): 72–81. https://doi.org/10.1016/j.palaeo.2006.11.036

Kolar-Jurkovšek, T., Jurkovšek, B., Aljinović, D., 2011a. Conodont Biostratigraphy and Lithostratigraphy across the Permian-Triassic Boundary at Lukač Section in Western Slovenia. *Rivista Italiana di Paleontologia e Stratigrafia*, 117: 115–133

Kolar-Jurkovšek, T., Jurkovšek, B., Aljinović, D., et al., 2011b. Stratigraphy of Upper Permian and Lower Triassic Strata of the Žiri Area (Slovenia). *Geologija*, 53(2): 193–204. https://doi.org/10.5474/geologija.2011.015

Kolar-Jurkovšek, T., Jurkovšek, B., 2015. Conodont Zonation of Lower Triassic Strata in Slovenia. *Geologija*, 58(2): 155–174. https://doi.org/10.5474/geologija.2015.012

Kolar-Jurkovšek, T., Jurkovšek, B., 2016. Conodont Zonation for the Lower Triassic of Western Tethys—A Case Study from Slovenia. The 5th International Geological Congress, August 27–September 4, 2016, Cape Town, South Africa

Kovács, S., Sudar, M., Karamata, S., et al., 2010. Triassic Environments in the Circum-Pannonian Region Related to the Initial Neotethyan Rifting Stage. In: Vozar, J., Ebner, F., Vozárova, A., et al., eds., Variscan and Alpine Terranes of the Circum-Pannonian Region. Slovak Academy of Sciences, Geological Institute, Bratislava. 87–156

Kreisa, R. D., 1981. Storm-Generated Sedimentary Structures in Subtidal Marine Facies with Examples from the Middle and Upper Ordovician of Southwestern Virginia. *SEPM Journal of Sedimentary Research*, 51: 832–849

Krainer, K., 1993. The Alpine Buntsandstein Formation of the Drau Range (Eastern Alps, Austria): Transition from Fluvial to Shallow Marine Facies. In: Lucas, S. G., Morales, M., eds., The Nonmarine Triassic. *New Mexico Museum of Natural History and Science Bull*., 3: 267–275

Krystyn, L., 1974. Die *Tirolites*-Fauna (Ammonoidea) der Untertriassischen Werfen Schichten Europas und Iher Stratigraphische Bedeutung. *Sitzberg. Oster. Akad. Wiss. Matem. -Naturw. Kl. Abt*., 193(1/2/3): 29–50

Krystyn, L., Balini, M., Nicora, A., 2004. Lower and Middle Triassic Stage Boundaries in Spiti. *Albertiana*, 30: 39–53

Krystyn, L., Đaković, M., Horacek, M., et al., 2014. Pelagically Influenced Late Permian and Early Triassic Deposits in Montenegro: Remnant of Internal Dinarid Neotethys or Paleotethys Relict? *Bericht des Institutes für Erdwissenschaften der Universität Graz*, 20(1): 114

Krystyn, L., Horacek, M., Brandner, R., et al., 2015. Carbon Isotopy as Major Chronostratigraphic Correlation Tool: The Early Triassic Case. *Bericht des Institutes für Erdwissenschaften der Universität Graz*, 21: 212

Lukasik, J. J., James, N. P., McGowran, B., et al., 2000. An Epeiric Ramp: Low-Energy, Cool-Water Carbonate Facies in a Tertiary Inland Sea, Murray Basin, South Australia. *Sedimentology*, 47(4): 851–881

Mostler, H., Rossner, R., 1984. Mikrofazies ünd Palökologie Der Höheren Werfener Schichten (Untertrias) der Nördlichen Kalkalpen. *Facies*, 10(1): 87–143. https://doi.org/10.1007/bf02536689

Nestell, G. P., Sudar, M. N., Jovanović, D., et al., 2009. Latest Permian Foraminifers from the Vlašić Mountain Area, Northwestern Serbia. *Micropaleontology*, 55: 495–513

Nestell, G. P., Kolar-Jurkovšek, T., Jurkovšek, B., et al., 2011. Foraminifera from the Permian-Triassic Transition in Western Slovenia. *Micropaleontology*, 57: 197–222

Payne, J. L., Lehrmann, D. J., Wei, J. Y., et al., 2004. Large Perturbations of the Carbon Cycle during Recovery from the End-Permian Extinction. *Science*, 305(5683): 506–509. https://doi.org/10.1126/science.1097023

Payne, J. L., Lehrmann, D. J., Wei, J., et al., 2006. The Pattern and Timing of Biotic Recovery from the End-Permian Extinction on the Great Bank of Guizhou, Guizhou Province, China. *Palaios*, 21(1): 63–85. https://doi.org/10.2110/palo.2005.p05-12p

Perri, M. C., 1991. Conodont Biostratigraphy of the Werfen Formation (Lower Triassic), Southern Alps, Italy. *Boll. Soc. Paleont. Ital.*, 30(1): 23–46

Perri, M. C., Andraghetti, M., 1987. Permian-Triassic Boundary and Early Triassic Conodonts from the Southern Alps, Italy. *Riv. It. Paleont. Strat*., 93: 291–328

Perri, M. C., Farabegoli, E., 2003. Conodonts across the Permian-Triassic Boundary in the Southern Alps. *Courier Forschungsinstitut Senckenberg*, 245: 281–313

Posenato, R., 2008. Patterns of Bivalve Biodiversity from Early to Middle Triassic in the Southern Alps (Italy): Regional vs. Global Events. *Palaeogeography*, *Palaeoclimatology*, *Palaeoecology*, 261(1/2): 145–159. https://doi.org/10.1016/j.palaeo.2008.01.006

Pratt, B. R., James, N. P., 1986. The St George Group (Lower Ordovician) of Western Newfoundland: Tidal Flat Island Model for Carbonate Sedimentation in Shallow Epeiric Seas. *Sedimentology*, 33(3): 313–343. https://doi.org/10.1111/j.1365-3091.1986.tb00540.x

Read, J. F., 1998. Phanerozoic Carbonate Ramps from Greenhouse, Transitional and Ice-House Worlds: Clues from Field and Modelling Studies. *Geological Society*, *London*, *Special Publications*, 149(1): 107–135. https://doi.org/10.1144/gsl.sp.1999.149.01.07

Read, J. F., Husinec, A., Cangialosi, M., et al., 2016. Climate Controlled, Fabric Destructive, Reflux Dolomitization and Stabilization Via Marine- and Synorogenic Mixed Fluids: An Example from a Large Mesozoic, Calcite-Sea Platform, Croatia. *Palaeogeography*, *Palaeoclimatology*, *Palaeoecology*, 449: 108–126. https://doi.org/10.13039/100000001

Reineck, H. E., Singh, I. B., 1972. Genesis of Laminated Sand and Graded Rhythmites in Storm-Sand Layers of Shelf Mud. *Sedimentology*, 18(1/2): 123–128. https://doi.org/10.1111/j.1365-3091.1972.tb00007.x

Retallack, G. J., 1995. Permian-Triassic Life Crisis on Land. *Science*, 267(5194): 77–80. https://doi.org/10.1126/science.267.5194.77

Retallack, G. J., 2005. Earliest Triassic Claystone Breccias and Soil-Erosion Crisis. *Journal of Sedimentary Research*, 75(4): 679–695. https://doi.org/10.2110/jsr.2005.055

Richoz, S., 2006. Stratigraphie et Variations Isotopiques du Carbone Dans le Permien Supérieur et le Trias Inferieur de Quelques Localités de la Néotéthys (Turquie, Oman et Iran). *Mémoire de Géologie de Lausanne*, 46: 275

Von Richthofen, F., 1860. Geognostische Beschreibung der Umgegend von Pedrazzo, St. Cassian und der Seiser Alpe in Südtirol, Gotha. 372

Romano, C., Goudemand, N., Vennemann, T. W., et al., 2013. Climatic and Biotic Upheavals Following the End-Permian Mass Extinction. *Nature Geoscience*, 6(1): 57–60. https://doi.org/10.1038/ngeo1667

Rüffer, T., Zühlke, R. 1995. Sequence Stratigraphy and Sea-Level Changes in the Early to Middle Triassic of the Alps: A Global Comparison. In: Haq, B. U., ed., Sequence Stratigraphy and Depositional Response to Eustatic, Tectonic and Climatic Foreing. Kluwer, Dordrecht. 161–207

Scotese, C. R., 2001. Atlas of Earth History. Palaeogeography, PalaeoMap Project, Arlington. 52

Song, H. J., Tong, J. N., Xiong, Y. L., et al., 2012. The Large Increase of $\delta^{13}C$ Carb-Depth Gradient and the End-Permian Mass Extinction. *Science China Earth Sciences*, 55(7): 1101–1109. https://doi.org/10.1007/s11430-012-4416-1

Stampfli, G. M., Borel, G., 2002. A Plate Tectonic Model for the Paleozoic and Mesozoic Constrained by Dynamic Plate Boundaries and Restored Synthetic Oceanic Isochrons. *Earth and Planetary Science Letters*, 196(1/2): 17–33. https://doi.org/10.1016/s0012-821x(01)00588-x

Stampfli, G. M., Hochard, C., Vérard, C., et al., 2013. The Formation of Pangea. *Tectonophysics*, 593: 1–19. https://doi.org/10.1016/j.tecto.2013.02.037

Sudar, M., Jovanović, D., Kolar-Jurkovšek, T., 2007. Late Permian Conodonts from Jadar Block (Vardar Zone, Northwestern Serbia). *Geologica Carpathica*, 58: 145–152

Sudar, M. N., Chen, Y. L., Kolar-Jurkovšek, T., et al., 2014. Lower Triassic (Olenekian) Microfauna from Jadar Block (Gucevo Mt., Nw Serbia). *Annales Geologiques de la Peninsule Balkanique*, 75: 1–15. https://doi.org/10.2298/gabp1475001s

Sun, Y. D., Joachimski, M. M., Wignall, P. B., et al., 2012. Lethally Hot Temperatures during the Early Triassic Greenhouse. *Science*, 338: 366–370

Sun, Y. D., Wignall, P. B., Joachimski, M. M., et al., 2015. High Amplitude Redox Changes in the Late Early Triassic of South China and the Smithian–Spathian Extinction. *Palaeogeography*, *Palaeoclimatology*, *Palaeoecology*, 427: 62–78. https://doi.org/10.13039/100007834

Šćavničar, B., 1973. Casts of Salt Crystals in Clastic Rocks in the Environs of Vrlika and Knin (Dalmatia). *Geol. Vjesnik*, 26: 155–157

Šćavničar, B., Šušnjara, A., 1983. The Geologic Column of the Lower Triassic at Muć (Southern Croatia). *Acta Geologica*, 13: 1–25

Tišljar, J., 1992. Origin and Depositional Environments of the Cvaporite and Carbonate Complex (Upper Permian) from the Central Part of the Dinarides (Southern Croatia and Western Bosnia). *Geol. Croatica*, 45: 115–127

Tollmann, A., 1976. Analyse des Klassischen Nordalpinen Mesozoikums. Monographie der Nördlichen Kalkalpen. Teil 2. Deuticke, Wien

Tucker, M. E., Wright, V. P., 1990. Carbonate Sedimentology. Blackwell Science Lit., Oxford. 482

Twitchett, R. J., 2006. The Palaeoclimatology, Palaeoecology and Palaeoenvironmental Analysis of Mass Extinction Events. *Palaeogeography*, *Palaeoclimatology*, *Palaeoecology*, 232(2/3/4): 190–213. https://doi.org/10.1016/j.palaeo.2005.05.019

Vlahović, I., Tišljar, J., Velić, I., et al., 2005. Evolution of the Adriatic Carbonate Platform: Palaeogeography, Main Events and Depositional Dynamics. *Palaeogeography*, *Palaeoclimatology*, *Palaeoecology*, 220(3/4): 333–360. https://doi.org/10.1016/j.palaeo.2005.01.011

Whiteker, J. H., McD., 1973. “Gutter Cast”, a New Name for Scour-and-Fill Structures: With Examples from the Llandoverian of Ringerike and Malmoya, Southern Norway. *Norsk Geologisk Tidsskrifl*, 53: 403–417

Wissman, H. L., Munster, G. V., 1841. Beitrage zur Geognosie und Petrefacten-Kundes des Sudestlich Tirol’s Vorzuglich der Schichten von St. Cassian. *Beiträge zur Petrefactenkunde*, 4: 1–152

Wright, V. P., Faulkner, T. J., 2010. Sediment Dynamics of Early Carboniferous Ramps: A Proposal. *Geological Journal*, 25(2): 139–144. https://doi.org/10.1002/gj.3350250205